RSC Advances

REVIEW

View Article Online
View Journal | View Issue

Cite this: *RSC Adv.*, 2014, **4**, 58826

Fundamental aspects of property tuning in push–pull molecules†

Filip Bureš*

Received 26th September 2014
Accepted 21st October 2014

DOI: 10.1039/c4ra11264d

www.rsc.org/advances

Property tuning in selected examples of D–π–A molecules has been discussed and summarized in this review article. The tuning and structure–property relationships have been demonstrated on the particular A, π and D parts of the push–pull molecule. Special emphasis has been put on the tuning of the FMO levels and optical properties. Further prospective applications of the given chromophore have also been considered.

1. Introduction

Nowadays, organic molecules with a delocalized π-system of electrons represent attractive targets for application in advanced functional materials. Due to their easy synthesis, well-defined and tuneable structure, molecular arrangement, and predictable, peculiar and unique properties, (hetero)aromatic π-conjugated systems are a notable feature of materials science. Within the last four or five decades, organic π-systems have become an extensively investigated, burgeoning area of organic chemistry, and have found widespread applications across various branches of modern research. They can be found as active substances in organic electronics and optoelectronics,[1] conductors,[2] photovoltaics[3] and solar photon conversion.[4] Based on the development in these fields, and in parallel to widely explored inorganic analogues, organic devices such as field-effect transistors (OFET),[5] light-emitting diodes (OLED),[6] photovoltaic cells (OPVC),[7] dye-sensitizing solar cells (DSSC)[8] and bulk-heterojunction solar cells (BHJ)[9] belong to well established and known applications of π-conjugated molecules.

Organic π-systems end-capped with an electron donor (D) and an electron acceptor (A) represent a subclass of the aforementioned molecules widely known as push–pull systems. D–A interaction, or so-called intramolecular charge-transfer (ICT), in such D–π–A molecules accounts for even more distinct optoelectronic properties. Due to the D–A interaction, a new low-energy molecular orbital (MO) is being formed. Facile excitation of the electrons within the new MO can be achieved using visible light, and therefore push–pull molecules are generally coloured and referred to as charge-transfer chromophores.[10] The ICT is also responsible for the polarization of the push–pull chromophore and generation of a molecular dipole. The extent of the ICT can be expressed by two limiting resonance forms, as shown in Fig. 1 for a simple D–π–A model based on nitroaniline. The impact of the ICT on the optical properties of π-conjugated molecules can be demonstrated by the UV/Vis absorption spectra measured for aniline, nitrobenzene, 4-nitroaniline and 3-nitroaniline (Fig. 1). Whereas for the first two compounds only absorption in the UV region is being observed, 4-nitroaniline showed intense and bathochromically shifted longest-wavelength absorption maxima (CT-band). On the contrary, 3-nitroaniline showed only a diminished CT-band as a result of a non-conjugating arrangement of the amino donor and the nitro acceptor.

Typical electron donors D are represented by the substituents with +M/+I effects such as OH, NH_2, OR and NR_2, heterocyclic moieties such as thiophene[11] and proaromatic pyran-4-ylidines[12] as well as some metallocenes.[13,14] On the other hand, the most used electron acceptors A involve substituents featuring −M/−I effects such as NO_2, CN, CHO and electron

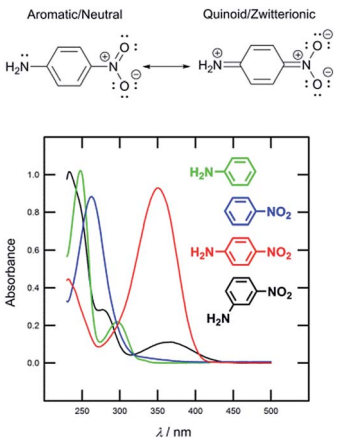

Fig. 1 Limiting resonance forms and UV/Vis spectra for model D–π–A systems based on nitroaniline.

Institute of Organic Chemistry and Technology, Faculty of Chemical Technology, University of Pardubice, Studentská 573, Pardubice, Czech Republic. E-mail: filip.bures@upce.cz; Web: http://bures.upce.cz; Fax: +420 46 603 7068; Tel: +420 46 603 7099

† Electronic supplementary information (ESI) available. See DOI: 10.1039/c4ra11264d

deficient heterocyclic compounds such as (di)azines,[15] benzothiazole[16] and imidazole.[17] Table 1 compares the electronic properties of selected electron withdrawing and donating groups used as A/D parts of push–pull molecules through the Hammett σ_p and Pytela σ^i substitution constants.[18]

The data in Table 1 rationalizes why substituents such as nitro/cyano and *N*,*N*-dimethylamino are among the strongest and most widely used electron acceptors and donors. Beside these groups, less common (perfluoro)sulfo(a)nyl and ferrocenyl groups also impart notable electronic effects (resonance and inductive) to push–pull molecules, as indicated by their high σ_p constants. Compared to *N*,*N*-dialkylamino ($\sigma_p = -0.83$), the increasingly popular *N*,*N*-diphenyl(aryl)amino group ($\sigma_p = -0.56$) possesses a lower donating ability, most likely due to a partial delocalization of the amine lone electron pair to the appended phenyls(aryls), which are generally arranged in a nonplanar manner. In modern push–pull chromophores, the π-conjugated path is created by a combination of multiple bonds (olefinic and acetylenic scaffolding)[10] and aromatic (mostly benzenoids)[10] or heteroaromatic spacers.[15,17] Push–pull molecules may adopt several arrangements. The most widely utilized are linear (D–π–A), quadrupolar (D–π–A–π–D or A–π–D–π–A) and octupolar/tripodal ($(D–\pi)_3$–A or $(A–\pi)_3$–D) systems. However, push–pull molecules were also reported with extraordinary arrangements such as V- (ref. 19), Y- (ref. 17), H- (ref. 20) and X-shapes.[21–23]

Besides the aforementioned general use of organic π-conjugated molecules, push–pull molecules found predominant applications as chromophores with nonlinear optical (NLO) properties,[24] electro-optic[25] and piezochromic[26] materials, NLO switches,[27] photochromic[28] and solvatochromic probes[29] as well as active layers in DSSCs.[8] The second- and third-order optical nonlinearities of push–pull molecules are mainly affected by the extent of the ICT, and thus result in polarization of the π-system.[30] In principle, the ICT and the corresponding HOMO–LUMO gap, optical properties and NLO response can be tailored by (i) attaching electron donors and acceptors of various electronic nature, (ii) assuring efficient D–A interaction, (iii) extension, composition and spatial arrangement of the π-linker, (iv) reducing the bond-length alternation (BLA) of the π-system and (v) planarization of the entire molecule.[31] Hence, in the following text will be reviewed recent examples of push–pull chromophores. The main purpose of this article is not to comprehensively review all available push–pull molecules but rather to demonstrate the fundamental principles of property tuning on suitable examples. Structural aspects and relationships mainly affecting the energies of the frontier molecular orbitals as well as the optical properties will be discussed. The influence of such tuning on the prospective application of the given chromophore will also be considered. The property tuning will be discussed according to the part of the D–π–A system involved (donor, π-system and acceptor).

Table 1 Comparison of electronic properties of selected groups used as acceptors and donors in push–pull chromophores

Acceptors			Donors		
Subst.	σ_p	σ^i	Subst.	σ_p	σ^i
NO_2	0.78	0.606	NMe_2	−0.83	0.089
CN	0.66	0.525	NHMe	−0.70	0.094
CHO	0.42	0.385	NH_2	−0.66	0.089
COMe	0.50	0.286	NHPh	−0.56	—
COPh	0.43	—	NPh_2	−0.22	—
COOH	0.45	0.264	OH	−0.37	0.157
COOMe	0.45	0.274	OMe	−0.27	0.220
CF_3	0.54	0.372	OPh	−0.03	0.278
$COCF_3$	0.80	—	SMe	0.00	0.217
C_6F_5	0.27	—	2-Thienyl	0.05	—
SO_2Me	0.72	0.551	Fc	−0.18	—
SO_2CN	1.26	—			
SO_2CF_3	0.96	—			
SF_5	0.68	—			
Pyridin-4-yl	0.44	—			
Benzoxazol-2-yl	0.33	—			
Benzothiazol-2-yl	0.29	—			

2. Tuning through the donor

The most widely employed electron donors in push–pull molecules involve functional groups possessing +M effect such as *N*,*N*-dialkylamino (typically *N*,*N*-dimethylamino), alkoxy groups (typically methoxy) as well as auxiliary electron donors, such as electron rich five-membered heteroaromates (typically thiophene) or organometallic compounds (typically ferrocene). The molecular properties of D–π–A systems can be tailored by its replacement (stronger/weaker), addition (one or more donors) or position (conjugating/nonconjugating arrangement) of the electron donor. In 2010, we published a series of donor-substituted D–π–A molecules **1–6** bearing a 1-methylimidazole-4,5-dicarbonitrile acceptor (dicyanoimidazole (DCI), Fig. 2).[32,17,30f] In this systematic study, property tuning has been achieved by increasing the donating ability of the appended donors (H < MeO < Me_2N) as well as the π-system extension. More recently, the series **a–c** have been completed by analogous compounds **d** bearing a ferrocenyl donor.[14a] The synthesis of compounds **1–6** involves Suzuki–Miyaura cross-coupling of donor substituted boronic acids or their pinacol esters[33] with a 2-bromo-DCI precursor. For a demonstration of the impact of the electron donor, we can select compounds **3a–d** bearing a styryl π-linker. Among others, the molecular structure and spatial arrangement of the methoxy and ferrocenyl substituted chromophores **3b** and **3d** are shown in Fig. 3. As can be seen, the DCI acceptor and the styryl linker adopt a planar arrangement, which assures an efficient D–A interaction. Electrochemically measured HOMO and LUMO levels and their differences E_g as well as the positions of the longest wavelength absorption maxima λ_{max} are summarized in Table 2. However, for better understanding, the data is also presented as an energy level diagram (Fig. 4) and a UV/Vis absorption spectrum (Fig. 5).

While the LUMO levels remained almost unaltered ($E_{LUMO} = -2.78$ to -2.62 eV), the principle changes were observed in the HOMO energies ($E_{HOMO} = -6.15$ to -4.87 eV). Considering the identical acceptor and the styryl π-system in all chromophores, the observed changes clearly reflect various electronic

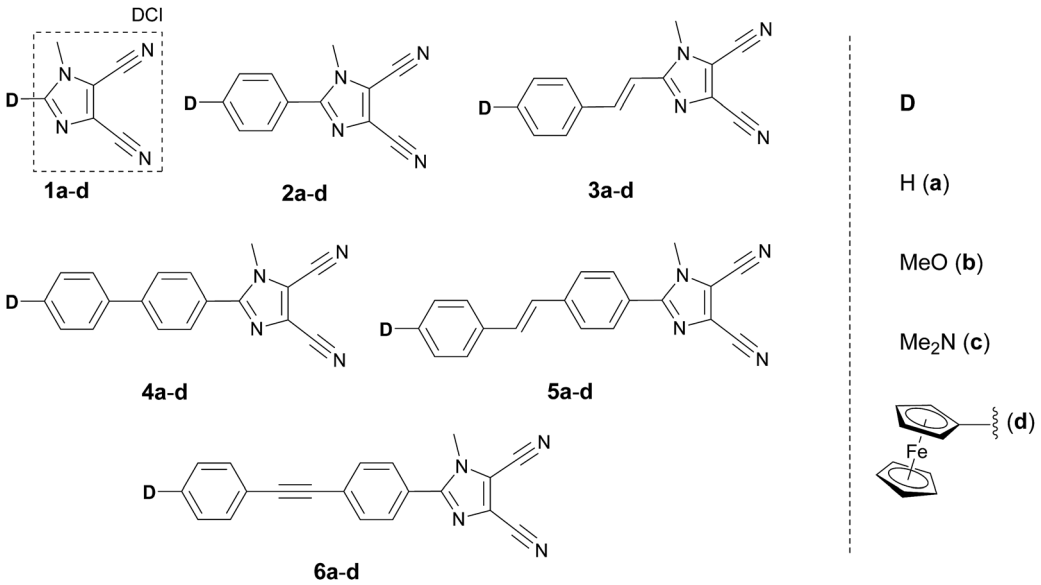

Fig. 2 Structure of DCI-derived push–pull molecules **1–6** with various electron donors.

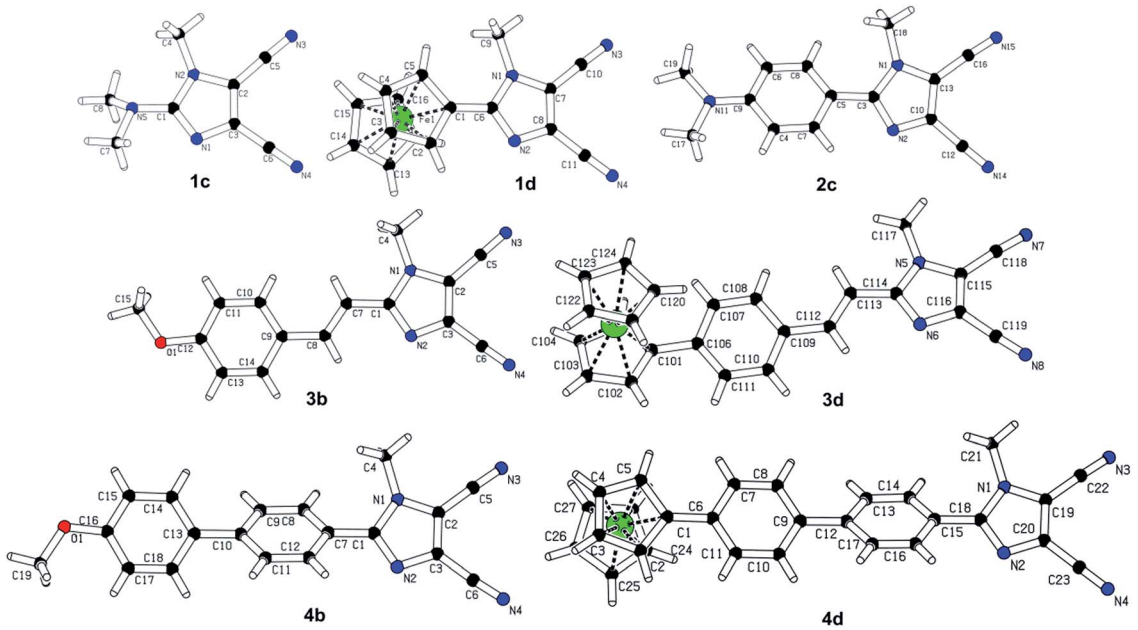

Fig. 3 Molecular X-ray structures of successfully crystallized chromophores from the series **1–6**.

Table 2 Optoelectronic properties of DCI-derived D–π–A systems **3a–d**

Comp.	D	E_{HOMO} [eV]	E_{LUMO} [eV]	E_g [eV]	$\lambda_{max}{}^c$ [nm (eV)]
3a	H	−6.15[a]	−2.78[a]	3.37	313(3.96)
3b	MeO	−5.76[a]	−2.68[a]	3.08	331(3.75)
3c	Me_2N	−5.12[a]	−2.62[a]	2.50	381(3.25)
3d	Fc	−4.87[b]	−2.67[b]	2.20	346(3.58)/472(2.63)

[a] Measured by CV, RDV and DC polarography in acetonitrile and recalculated.[34] [b] Measured by CV and RDV in DMF and recalculated.[34] [c] Measured in dichloromethane at $c = 10^{-5}$ M.

behaviours of the appended donors. Replacement of the hydrogen in **3a** by a methoxy group (**3b**) shifted the HOMO–LUMO gap from 3.37 to 3.08 eV (Fig. 4). Further addition of donors such as the *N*,*N*-dimethylamino (**3c**) or ferrocenyl (**3d**) groups resulted in the decrease of E_g to 2.50 and 2.20 eV, respectively. Hence, the HOMO level and thus resulting E_g of a given acceptor substituted π-system can be tuned very easily and efficiently by a variation of the donor ($\Delta E_g = 1.17$ eV). The DFT-derived HOMO and LUMO in chromophore **3c** are visualized in Fig. 4.[35] As expected, the HOMO is localized on the donating *N*,*N*-dimethylanilino moiety, while the LUMO is

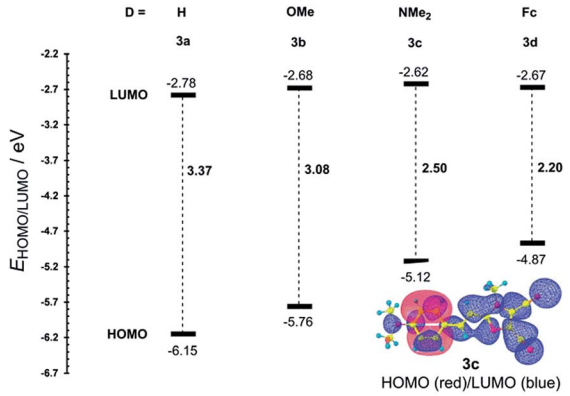

Fig. 4 Energy level diagram showing HOMO/LUMO levels of **3a–d**.

centred on the DCI acceptor and the adjacent part of the π-linker. The UV/Vis absorption spectra of **3a–d** are dominated by intensive CT-bands appearing between 313 and 381(472) nm (Table 2, Fig. 5). By increasing the donating strength of the appended donors in the order H < MeO < Me_2N, the position of the CT-band shifted bathochromically by 19 and 50 nm. The ferrocene donor showed two particular CT-bands. The intense high-energy band appearing at 346 nm corresponds to the HOMO-3 → LUMO interaction (cyclopentadienyl → DCI); the weak low-energy band at 472 nm originates from the interaction between the Fe-centred HOMO and the DCI-centred LUMO.[14a] Hence, ferrocene must be considered as a donor featuring dual ICT of various efficiencies. However, the optical properties of a push–pull chromophore can be tuned through the donor in a similar manner to their HOMO–LUMO gaps.

In the 90s, very nice examples of property tuning in push–pull molecules by variation of the donors were also demonstrated by Würthner *et al.*,[36] Perry *et al.*/Brédas *et al.*[37] and Marder *et al.*[38] Würthner demonstrated substituent variation on a 2,2′-bithiophene scaffold **7a–e** end-capped with a nitro acceptor, Perry and Brédas focused experimentally/theoretically on the donor–acceptor diphenylacetylenes **8a–e** and Marder showed highly polarizable push–pull imines based on 2,6-di-*tert*-butylindoanilines **9a–f** (Fig. 6). All these push–pull molecules were investigated as efficient NLO phores (Table 3). Electron donors are represented by the hydrogen, bromo, methoxy, methylthio, amino, *N*-methylamino, *N*,*N*-dimethylamino and 1-pyrrolidino (PyN) groups. Optoelectronic properties of push–pull molecules **7–9** were evaluated by means of their ground state dipole moment μ, its change upon excitation $\Delta\mu$, the position of the longest-wavelength absorption maxima (including solvatochromism), as well as the first molecular hyperpolarizability β_0 (EFISH). As a general trend, bathochromic shift of the CT-band, raised dipole moment and its change upon excitation and increased magnitude of β_0 have been observed with increasing donor strength. The most bathochromically shifted λ_{max} and highest nonlinear optical responses were measured for push–pull molecules bearing a *N*,*N*-dimethylamino donor. In any case the high donating character of pyrolidin-1-yl as in **7e** should not be neglected. Two methoxy groups attached at the conjugated positions 2 and 4 (**9e** *vs.* **9d**) caused an additional bathochromic shift of 29 nm, however the impact on the first hyperpolarizability is diminished. The MeS donor seems to be slightly more efficient than MeO. It red-shifts the CT-band similarly to MeO, however, due to the presence of the polarizable sulphur atom, NLO phores **7c**,

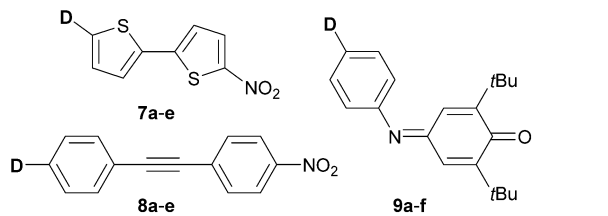

Fig. 6 Push–pull 2,2′-bithiophenes **7**, diphenylacetylenes **8** and 2,6-di*tert*butylindoanilines **9**.

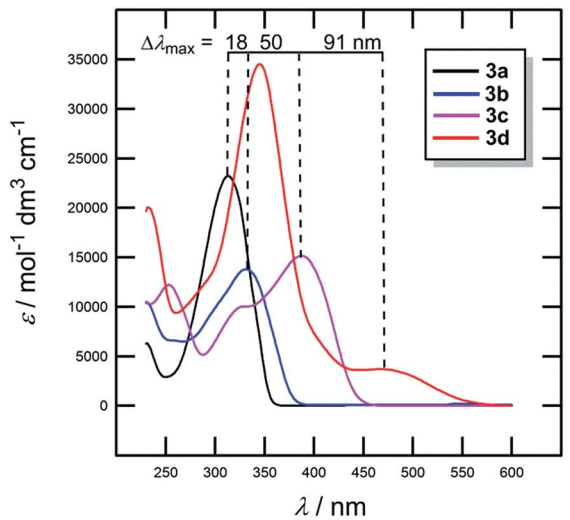

Fig. 5 UV/Vis absorption spectra of chromophores **3a–d**.

Table 3 Push–pull molecules **7–9** – properties

Comp.	D	μ_g [D]	$\Delta\mu$ [D]	λ_{max} [nm (eV)]	$\beta_0{}^c$ [10^{-30} esu]
7a	H	5.04[a]	7.55	375(3.31)[b]	9.4
7b	MeO	6.03[a]	11.35	408(3.04)[b]	18.9
7c	MeS	4.98[a]	16.31	391(3.17)[b]	26.9
7d	Me_2N	7.93[a]	13.96	466(2.66)[b]	41.0
7e	PyN	8.41[a]	16.47	499(2.48)[b]	56.0
8a	MeO	4.40	6.20	347(3.57)[d]	14.0
8b	MeS	4.00	5.40	358(3.46)[d]	20.0
8c	H_2N	5.50	9.50	379(3.27)[d]	24.0
8d	MeHN	5.70	7.70	400(3.10)[d]	46.0
8e	Me_2N	6.10	5.70	416(2.98)[d]	46.0
9a	H	1.5[e]	—	428(2.90)[d]	4.5
9b	Br	1.3[e]	—	432(2.87)[d]	9.9
9c	MeS	2.3[e]	—	476(2.61)[d]	11.0
9d	MeO	2.4[e]	—	469(2.64)[d]	12.0
9e	2,4-DiMeO	3.4[e]	—	498(2.45)[d]	13.0
9f	Me_2N	3.9[e]	—	558(2.22)[d]	47.0

[a] Measured in benzene. [b] Measured in *n*-hexane. [c] EFISH experiment (1910 nm). [d] Measured in chloroform. [e] [10^{-30} esu].

8b and **9c** undergo large changes in the dipole moment upon excitation and are slightly more polarized than **7b**, **8a** and **9d** (Table 3). Besides the aforementioned contributions, Marder, Brédas, Perry, Cheng and others have developed the concept of a well-balanced donor/acceptor/π-system, which proved to be very crucial for the optimization of the NLO performance of organic D–π–A systems.[39]

More recently, Blanchard-Desce *et al.* reported NLO-active donor–acceptor polyenes **10a–c** and push–pull arylbithiophenes **11a–c** with efficient fluorescence and two-photon absorption (Fig. 7).[40] Both π-conjugated scaffolds were end-capped with *N*,*N*′-diethylthiobarbituric acid as an acceptor, while H, MeO, Me_2N, *N*,*N*-dibutylaninilo, julolidine, and 5-(piperidin-1-yl)thiophene-2-yl (PIT) groups were employed as electron donors.

Table 4 demonstrates that both absorption and emission maxima of polyenes **10** and arylbithiophenes **11** are red-shifted with increasing donor strength. However, the first hyperpolarizability of **10a–c** decreased from 150 to 55 × 10^{-30} esu.

According to Blanchard-Desce,[40a] this is a consequence of reduced BLA in polyenals with the π-system length as in **10a–c** (less balanced D–π–A NLO phore, for the BLA optimization see the further text). In contrast to polyenes **10**, arylbithiophenes **11** showed a significant increase in fluorescence and large one- and two-photon brightness reaching the TPA cross-section of 1180 GM, measured for **11c**. Hence, arylbithiophenes **11** hold promise as biphotonic fluorescent probes for bioimaging.

Tuning of the donor in TPA-active push–pull chromophores **12** has also been demonstrated by Abbotto *et al.* (Fig. 7).[41] They have investigated simple pyridinium salts **12a–e** linked to electron rich pyrrole (donor), which was further substituted by methyl and phenyl groups. The pyrrole electron releasing ability and the corresponding ICT and optical properties were finely tuned by minor structural changes, which, however, have a significant impact on frequency up-converted lasing. Hence, chromophores **12a–e** were able to convert easily available infrared laser radiation at 790 nm into more useful visible laser emission over a wide region of the visible spectrum (522–576 nm) *via* a two-photon absorption-induced fluorescence phenomenon.

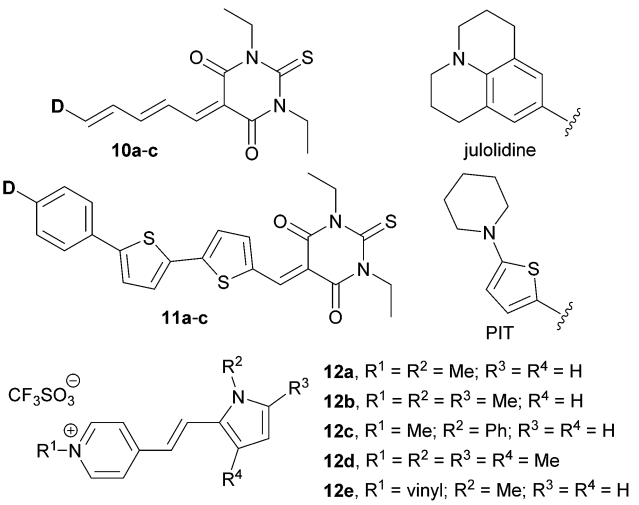

Fig. 7 Donor–acceptor polyenes **10**, arylbithiophne **11** and pyrrole-pyridinium chromophores **12**.

Table 4 Properties of polyenes **10a–c** and arylbithiophenes **11a–c**

Comp.	D	λ^{A}_{max} [a] [nm (eV)]	λ^{E}_{max} [a] [nm (eV)]	E_g [b] [eV]	NLO
10a	$Bu_2NC_6H_4$	587	—	1.68	150[c]
10b	Julolidine	614	—	1.54	130[c]
10c	PIT	619	—	1.54	55[c]
11a	H	527	596	—	—
11b	MeO	541	644	—	—
11c	Me_2N	588	781	—	1180[d]

[a] Measured in chloroform. [b] Measured by CV in acetonitrile (*vs.* SCE). [c] β_0 values measured by EFISH experiment (1907 nm) in chloroform [10^{-30} esu]. [d] TPA cross-section at 1100 nm in chloroform [GM].

Table 5 DFT-calculated properties of dye-sensitizer **13** and **14**

Comp.	E_{HOMO} [eV]	E_{LUMO} [eV]	E_g [eV]	λ_{max} [nm (eV)]
13a	−5.29[a]	−2.73[a]	2.56[a]	481(2.58)[a,b]
13b	−4.81[a]	−2.66[a]	2.15[a]	523(2.37)[a,b]
13c	−4.77[a]	−2.67[a]	2.10[a]	523(2.37)[a]
14a	−5.27[c]	−2.61[c]	2.66[c]	430(2.88)[c]
14b	−5.15[c]	−2.65[c]	2.50[c]	429(2.89)[c]
14c	−5.14[c]	−2.69[c]	2.45[c]	428(2.90)[c]
14d	−4.96[c]	−2.57[c]	2.39[c]	441(2.81)[c]
14e	−4.78[c]	−2.54[c]	2.24[c]	453(2.74)[c]

[a] DFT calculation in THF (CAM-TD-B3LYP/MPW1K). [b] Experimental λ_{max} values for **13a** and **13b** in THF are 502(2.47) and 523(2.37) nm (eV). [c] DFT calculation in vacuum (CAM-TD-B3LYP/6-31 G(d,p).

A proper selection of the donor part of the organic push–pull molecule is also currently a common strategy to improve the performance of the dye-sensitizer in DSSCs. In this respect, arylamines belong undoubtedly to the most widely employed electron-donor moieties.[8] Zhang *et al.*[42] and Jungsuttiwong *et al.*[43] have theoretically investigated organic dyes **13** and **14** with various peripheral donors based on a combination of carbazole, triphenylamine and bisfluorenyl moieties (Fig. 8 and Table 5).

Both dye-sensitizers **13** and **14** possess a good TiO_2-anchoring group (cyanoacrylilic acid) and well-tuned HOMO and LUMO. Whereas the LUMO levels are sufficiently negative with respect to the conduction band of TiO_2 (∼3.2 eV), the HOMO levels are close to the redox potential of the iodide/triiodide couple for efficient dye regeneration. In contrast to the recent concept of D–A–π–A systems,[8a] new dye-sensitizers **13** and **14** represent D–D–π–A push–pull molecules. As a general trend, we can observe that the absorption edge of the dye shifts bathochromically and the HOMO level and the corresponding E_g decreases with increasing number and electron releasing ability of the auxiliary donors. The donating ability of carbazole is generally weaker than that of triphenylamine (*e.g.* molecules **13a** *vs.* **13b** or **14c** *vs.* **14e**).

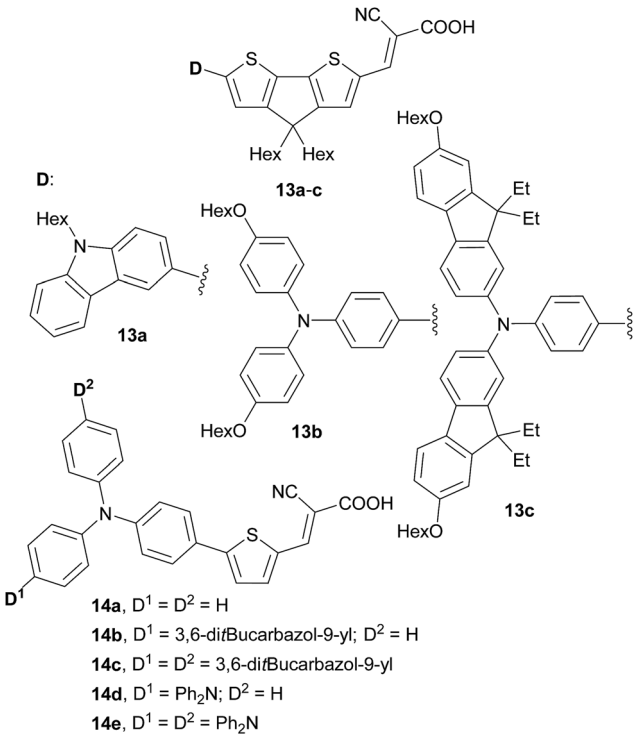

Fig. 8 Donor tuning in dye-sensitizers **13** and **14**.

3. Tuning through the π-system

The π-conjugated bridge between the electron donor and acceptor is an integral part of the D–π–A system and, therefore, its influence on the optoelectronic properties will be discussed herein. The π-linker consists of a combination of multiple bonds, aromates and heteroaromates and the basic structure–property relationships can be demonstrated on the *N*,*N*-dimethylamino substituted DCI molecules **1c–6c** shown in Fig. 2. Whereas molecule **1c** has the donor connected directly to the DCI acceptor, in chromophores **2c–6c** both moieties are separated by an additional π-linker such as 1,4-phenylene (**2c**), styryl (**3c**), biphenyl (**4c**), stilbenyl (**5c**) and phenylethynylphenyl (**6c**). The X-ray analyses in Fig. 3 show that particular π-linkers adopt various spatial arrangements. The five-membered DCI unit connected directly to 1,4-phenylene as in chromophores **2** and **4** adopts a nonplanar arrangement with a torsion angle of 29–33°.

Moreover, both 1,4-phenylene moieties of the biphenyl linker (**4**) are highly twisted. On the other hand, additional olefinic/acetylenic units as in **3**, **5** and **6** caused (partial) planarization of the entire π-system. The HOMO/LUMO and λ_{max} values of molecules **1c–6c** are summarized in Table 6 and Fig. 9 and 10.

As can be seen from Fig. 9, the most significant changes are observed in the HOMO levels. Extension of the π-system by one

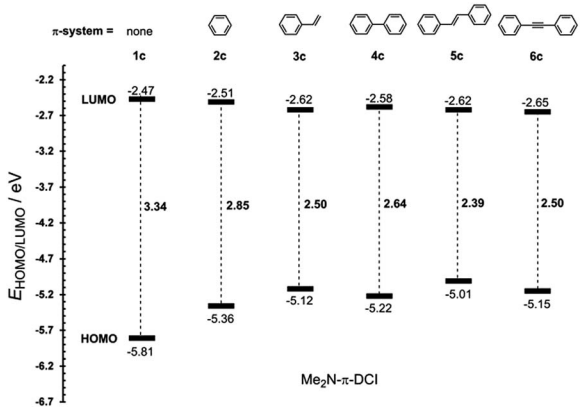

Fig. 9 Energy level diagram of **1c–6c** with systematically enlarged π-linker.

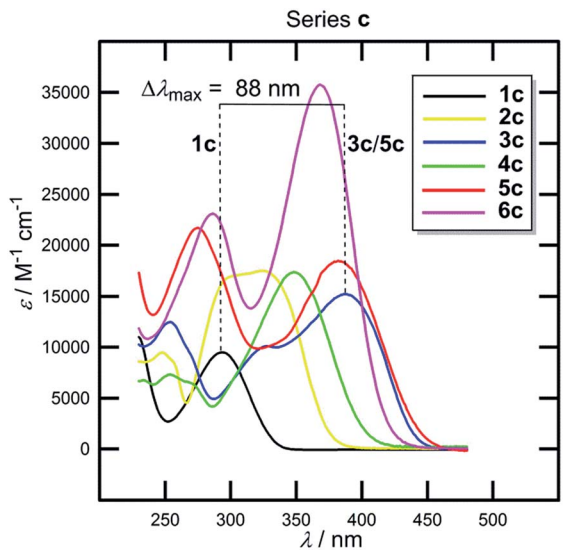

Fig. 10 UV/Vis absorption spectra of **1c–6c**.

Table 6 Optoelectronic properties of Me_2N–π–DCI systems **1c–6c**

Comp.	E_{HOMO} [a] [eV]	E_{LUMO} [a] [eV]	E_g [a] [eV]	λ^{A}_{max} [b] [nm (eV)]	λ^{E}_{max} [b] [nm (eV)]	β_{HRS} [c] [10^{-30} esu]
1c	−5.81	−2.47	3.34	293(4.23)	—	—
2c	−5.36	−2.51	2.85	316(3.92)	460(2.70)	19.2
3c	−5.12	−2.62	2.50	381(3.25)	474(2.62)	28.5
4c	−5.22	−2.58	2.64	346(3.58)	504(2.46)	26.3
5c	−5.01	−2.62	2.39	380(3.26)	533(2.33)	28.0
6c	−5.15	−2.65	2.50	364(3.41)	515(2.41)	40.4

[a] Measured by CV, RDV and DC polarography in acetonitrile and recalculated.[34] [b] Measured in dichloromethane. [c] HRS experiment in dichloromethane (1064 nm).

1,4-phenylene moiety (**1c** → **2c**) lowered the HOMO–LUMO gap by 0.49 eV. Further insertion of an olefinic unit between the DCI and 1,4-phenylene parts of the π-linker (**2c** → **3c**) resulted in a drop in E_g by an additional 0.35 eV. Despite being longer than styryl, the nonplanar bihenyl π-linker in **4c** allows less D–A interaction and, therefore, the HOMO–LUMO gap is raised to 2.64 eV. However, the gap can be lowered by planarization of the π-linker by olefinic or acetylenic units as in **5c** and **6c**. A comparison of **5c** and **6c** also allowed a demonstration of the "transparency" of the double and triple bond. The HOMO–LUMO gap of **5c** is lower by 0.11 eV compared to **6c**, which leads to the assumption that, in contrast to a vacuum,[44] the olefinic unit allows a higher D–A interaction than the acetylenic one. Hence, the most efficient ICT has been achieved in molecules **2c** and **5c** bearing fully-planar and transparent styryl and stilbenyl π-systems.

Now we can analyse the UV/Vis absorption spectra of **1c–6c** (Fig. 10, Table 6). With the same donor and acceptor, all observed changes must be attributed to the π-linker.

The position of the CT-bands ranges from 293 to 381 nm and is clearly dependent on the length, composition and spatial arrangement of the π-system. Similar trends as seen by the electrochemical measurements can also be concluded from the UV/Vis spectra. Moreover, both the optical and electrochemical gaps showed a very tight correlation (Fig. S1, ESI†). Thus, in **1c–6c** we can easily modulate the HOMO–LUMO gap and the position of the longest wavelength absorption maxima within the range of 0.95 eV and 88 nm by the extension and variation of the π-system between the *N*,*N*-dimethylamino donor and the DCI acceptor. Chromophores **1c–6c** were used as efficient NLO phores with tunable optical nonlinearities, pH- and photo-induced NLO switches and fluorophores (Table 6).[35,45]

Property tuning through the extension of the π-system has also been demonstrated on polyenes and polyynes, as shown for example on molecules **10** (Fig. 7)[40a] and **8** (Fig. 6).[37] Systematic extension of the central polye(y)ne π-system led to lower electrochemical as well as optical gaps E_g. However, it was demonstrated that the nonlinear optical response depends on the degree of BLA.[39d] The BLA can be defined as the difference between the average C–C single and multiple bond lengths in the conjugated backbone and arises from the mixing of limiting resonance forms (aromatic *vs.* quinoid, Fig. 1). Hence, the highest NLO activity was encountered for NLO phores with optimized donor–acceptor strengths and BLA (*e.g.* **10a** analogue with five double bonds possesses a β_0 coefficient of 1000 × 10^{-30} esu, Fig. 7).[40a] The structure–property relationships in polye(y)nic chromophores were also intensively studied by DFT calculations and various functions and benchmarks were developed to optimize their NLO response.[46]

Polyenes end-capped with *N*,*N*-dibutylanilino/tetrathiafulvalene donors and dicyanovinyl/thiobarbituric acceptors **15** and **16a–c** were investigated by Kelly *et al.*[47] and Garín *et al.* (Fig. 11, Table 7).[48] Compound **15** has been used as a model push–pull chromophore to investigate the effect of polyenic *vs.* aromatic π-linkers by resonance Raman intensity analysis. It was suggested that the two-state model is more appropriate for polyenic than aromatic chromophores.

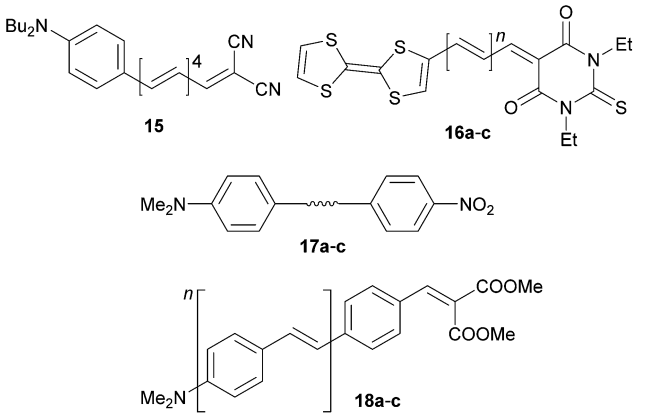

Fig. 11 Structure of oligomeric push–pull chromophores **15–18**.

Chromophores **16** showed a very narrow HOMO–LUMO band gap of 1.23–1.08 eV. Extension of the polyene backbone caused notable changes in the LUMO energies ($E_{red,1}$, Table 7) and thus decreased the E_g. The observed huge hypsochromic shift with $\Delta\lambda_{max} = 70$ nm is very unusual and was not explained. The very low solubility of **16a–c** in nonpolar solvents and unavoidable measurements in DMSO would play a significant role. In any case the NLO response ($\mu\beta_0$ product) is clearly a function of the number of double bonds in the conjugated backbone.

Acetylenic, olefinic and azo units are widely used features of π-linkers. Moylan *et al.* have reported (non)linear optical properties of simple push–pull molecules **17a–c** (Fig. 11, Table 7).[49] When going from **17a** to **17b** and **17c**, the CT-bands move bathochromically but the highest NLO response (β_0) has been recorded for the **17b** bearing olefinic unit. The azo linker in **17c** must, however, be considered as an auxochrome, which artificially red-shifts the CT-band. Despite the higher general polarizabilities of olefinic and azo π-linkers, their facile isomerization and generally lower stability also makes the acetylenic unit well-balanced in terms of polarizability, stability and synthetic accessibility (*e.g. via* Sonogashira cross-coupling).

Table 7 Selected properties of chromophores **15–18**

Comp.	Structure	$E_{ox,1}$ [V]	$E_{red,1}$ [V]	E_g [eV]	λ_{max} [nm (eV)]	NLO
16a	$n = 0$	0.60[a]	−0.63[a]	1.23	716(1.73)[b]	180[c]
16b	$n = 1$	0.60[a]	−0.57[a]	1.17	661(1.88)[b]	347[c]
16c	$n = 2$	0.56[a]	−0.52[a]	1.08	646(1.92)[b]	455[c]
17a	C≡C	—	—	—	416(2.98)[d]	32.8[e]
17b	CH=CH	—	—	—	438(2.83)[d]	42.1[e]
17c	N=N	—	—	—	480(2.58)[d]	39.9[e]
18a	$n = 0$	—	—	—	369(3.36)[f]	120[g]
18b	$n = 1$	—	—	—	410(3.02)[f]	170[g]
18c	$n = 2$	—	—	—	418(2.97)[f]	350[g]

[a] Measured by CV *vs.* Ag/AgCl in CH_2Cl_2/DMF. [b] Measured in DMSO. [c] $\mu\beta_0$ product measured by EFISH experiment (1907 nm) in DMSO [10^{-48} esu]. [d] Measured in chloroform. [e] β_0 measured by EFISH experiment (1907 nm) in chloroform [10^{-30} esu]. [f] Measured in toluene. [g] $\mu\beta_0$ product measured by EFISH experiment (1907 nm) in chloroform [10^{-48} esu].

Pasini *et al.* reported on crescent oligo-*p*-phenylenevinylene (PPV) type push–pull chromophores **18a–c** (Fig. 11). *N*,*N*-Dimethylamino and the less common dimethylmalonate groups were used as donor and acceptor, respectively.[50] As expected, the chromophores showed bathochromically shifted λ_{max} and enhanced NLO response with increasing number of styryl units. Whereas **18a** bearing the shortest π-linker showed a strong emission in the solid state, the emissions of the extended homologues **18b–c** were significantly quenched by aggregation (π-stacking). High quantum yield photoluminescence can be restored in the solution (toluene).

Diederich *et al.* and Biaggio *et al.*[22d,51] reported on the synthesis and third order optical nonlinearities of X-shaped donor-substituted cyanoethynylethenes **19** (Fig. 12). Property tuning has been achieved by a systematic extension of the central π-conjugated backbone by olefinic and acetylenic units and additional dicyanovinyl (DCV)[30f] acceptor moieties.

As can be seen from the data given in Table 8, an extension of the π-system in DsCEEs reduces the LUMO level ($E_{red,1}$). Hence, the electrochemically measured HOMO–LUMO gap decreases from 2.55 to 1.49 eV. A beneficial role of an additional acetylene unit ($n = 1$, Fig. 12) separating *N*,*N*-dimethylanilino (DMA) donors from the central conjugated backbone and causing planarization of the entire π-system is also noticeable (compare for instance **19a**/**19b** or **19c**/**19d**). Introduction of an additional DCV substituted branch ($k = 1$) as in **19g** and **19h** resulted in a further drop in the E_g to 1.49 eV. The optical band gap is red-shifted from 2.86 eV (434 nm) to 1.77 eV (700 nm). Thus, extension of the parent CEE scaffold in **19a**/**19b** by properly placed acetylenic and olefinic units caused huge tuning of $E^{el\text{-}chem/optical}_g$ by 1.06/1.09 eV (for the correlation of both gaps see Fig. S2, ESI†). Third-order polarizabilities γ_{rot} measured by degenerate four-wave mixing showed very similar trends as seen for electrochemical and optical gaps. X-shaped chromophore **19h** with two DMA and DCV units showed the third-order NLO response of $45 \pm 20 \times 10^{-23}$ m^5 V^{-2} kg^{-1}, which is one of the largest intrinsic second hyperpolarizabilities ever measured.[30a]

Brédas *et al.*[52] have theoretically investigated the influence of the nature of the π-linker on two-photon absorption of quadrupolar molecules **20a–f** (Fig. 13, Table 9). The cyano/*N*,*N*-dimethylamino acceptors/donors were appended to the π-

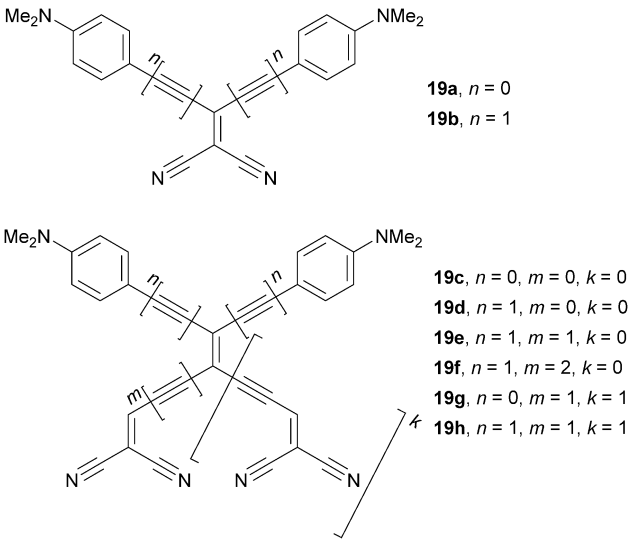

Fig. 12 Donor-substituted cyanoethynylethenes **19** (DsCEEs).

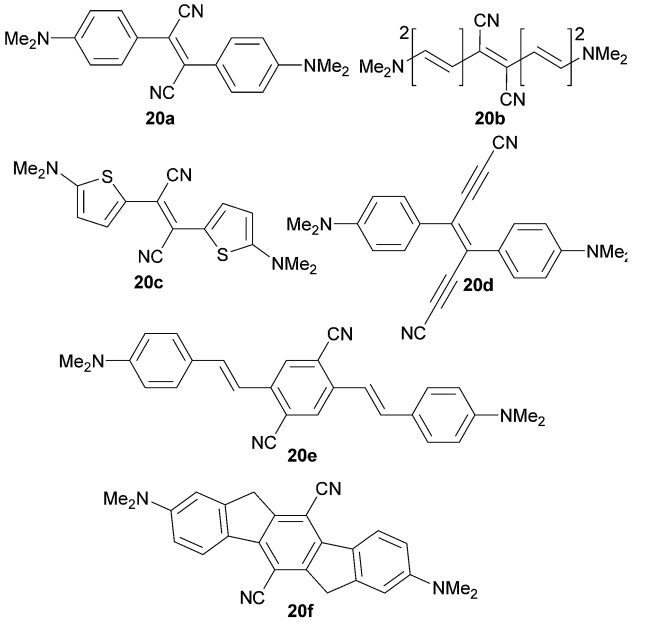

Fig. 13 Two-photon absorbing quadrupolar molecules **20a–f**.

Table 8 X-shaped push–pull molecules based on CEE **19**

Comp.	$E_{ox,1}$[a] [V]	$E_{red,1}$[a] [V]	E_g [eV]	λ_{max}[b] [nm (eV)]	γ_{rot}[c] [10^{-23} m^5 V^{-2} kg^{-1}]
19a	0.65	−1.90	2.55	434(2.86)	2 ± 2
19b	0.60	−1.34	1.94	524(2.37)	14 ± 3
19c	0.52	−1.71	2.23	498(2.49)	4 ± 3
19d	0.53	−1.25	1.78	534(2.32)	18 ± 5
19e	0.40	−1.18	1.58	580(2.14)[d]	13 ± 3
19f	0.46	−1.07	1.53	600(2.07)[d]	33 ± 15
19g	0.51	−1.38	1.89	632(1.96)	8 ± 4
19h	0.53	−0.96	1.49	700(1.77)[d]	45 ± 20

[a] Measured by CV/RDV *vs.* Fc^+/Fc couple in dichloromethane. [b] Measured in dichloromethane. [c] Third-order polarizability (second hyperpolarizability) measured by DFWM experiment (1500 nm) in dichloromethane. [d] Hidden peak maxima (deconvolution).

Table 9 Calculated properties of quadrupolar molecules **20a–f**

Comp.	M_{ge}[a] [D]	E_{ge}[a] [eV]	$M_{ee'}$[b] [D]	$E_{ge'}$[c] [eV]	δ_{approx}[d] [GM]
20a	8.51	3.22	12.85	3.79	512
20b	10.52	3.08	13.96	4.00	1560
20c	9.28	2.65	11.91	3.59	1119
20d	8.06	3.14	11.07	3.75	365
20e	11.27	3.34	17.22	3.87	1486
20f	7.53	3.41	12.40	4.12	429

[a] Transition dipoles/energies between the ground state (g) and intermediate one-photon state (e). [b] Transition dipoles between one- (e) and two-photon (e′) states. [c] Transition energies between ground state (g) and two-photon (e′) states. [d] TPA cross-section.

conjugated backbones comprising of phenylenevinylene (**20a** and **20d–e**), thienylenevinylene (**20c**), polyene (**20b**) and indenofluorene (**20f**) units. Table 9 summarizes one- and two-photon absorption properties (transition dipoles and energies). The calculated TPA cross-sections were dominantly dependent on the ground state polarization given by the quantities *M* and *E*. In general, molecules with large transition dipoles and lower transition energies delivered a stronger TPA response. Starting from **20a** (stilbene π-linker), switching to the polyenic π-system (**20b**), less aromatic thiophenes (**20c**) or elongation/planarization of the π-linker (**20e**) allows for an increase in δ by a factor of 2–3. On the other hand, extension or geometry restrictions of the π-system by two additional acetylenic units (**20d**) or indenofluorene backbone (**20f**) have a diminished effect.

4. Heteroaromatic π-systems

Besides the commonly used aromates (benzenoids) and multiple bonds, the π-conjugated backbone of push–pull molecules can also be constructed from heteroaromates. In recent years, D–π–A systems based on heteroaromatic scaffolding have attracted considerable attention of organic and material chemists.[15,17,53] It has been realized that incorporation of a heterocyclic moiety into the chromophore backbone leads to the following:

- higher chemical and thermal robustness
- auxiliary electron donor or acceptor effects
- considerably enhanced polarizability
- conformational stability
- non-centrosymmetry
- acid–base and chelating properties
- easy synthesis and further modification
- improved solubility
- possible biological properties

In this respect, thiophene is undoubtedly among the most explored five-membered heterocyclic moieties, and has already found manifold applications in modern organic electronics and photonics.[11] In 2012, we have investigated the extent of D–A interaction over the two most popular π-conjugated units – 1,4-phenylene and 2,5-thienylene π-linkers.[54] A series of fifteen model compounds bearing a ferrocene donor and nitro acceptor have been synthesized and further investigated by

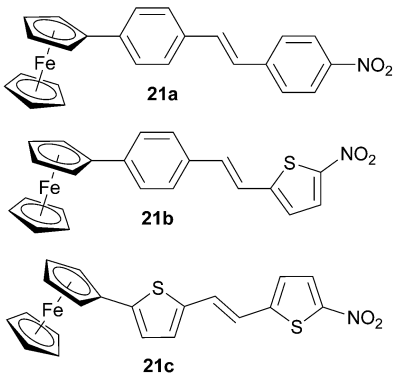

Fig. 14 Fc-π-NO_2 model push–pull molecules.

crystallography, electrochemistry, UV/Vis spectra and calculations. In the chosen chromophores **21a–c** (Fig. 14), the 1,4-phenylene units were systematically replaced with the 2,5-thienylene ones.

In contrast to the raised HOMO level caused by the extension and planarization of the π-system (see Fig. 9), gradual replacement of 1,4-phenylene moieties with 2,5-thienylene ones mainly lowered the LUMO levels (Fig. 15, Table 10). Hence, replacement of the first 1,4-phenylene unit resulted in a decrease of E_g from 1.51 to 1.34 eV. Replacement of the second 1,4-phenylene unit affected the HOMO–LUMO gap only negligibly. However, going from **21a** → **21b** → **21c**, the absorption spectra (Fig. 16) showed a gradual red-shift by 52/28 and 24/29 nm. Moreover, the intensity (ε) of the weakly observed LE band (Fe → NO_2/HOMO → LUMO transition) in **21a** increased by 3200 and 5700 M^{-1} cm^{-1}, respectively. Chromophore **21c**, bearing two thiophene rings with the highest ground-state and vertically-excited state dipole moments showed the most bathochromically shifted and pronounced CT-band with $\lambda_{max}^{LE} = 525$ nm.

Thiophene as a part of the π-system of push–pull molecules has also been investigated by Rao *et al.*[55] Dialkylamino and DCV end-capped push–pull molecules **22a–f** (Fig. 17) were investigated as tunable NLO phores. The property tuning has been achieved either by replacement of one or both 1,4-phenylene moieties in the parent molecule **22a** (→ **22c** → **22f**) or by

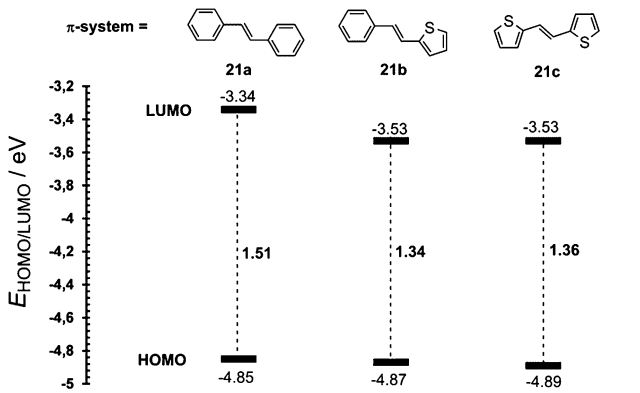

Fig. 15 Energy level diagram of **21a–c**.

Table 10 1,4-Phenylene *vs.* 2,5-thienylene π-linkers

Comp.	E_{HOMO}[a] [eV]	E_{LUMO}[a] [eV]	E_g[a] [eV]	$\lambda_{max}^{HE/LE}$[b] [nm (eV)]	μ_{gs}[c] [D]	μ_{ves}[c] [D]
21a	−4.85	−3.34	1.51	374(3.32)/472(2.63)	9.08	11.53
21b	−4.87	−3.53	1.34	426(2.91)/496(2.50)	10.77	14.91
21c	−4.89	−3.53	1.36	454(2.73)/525(2.36)	11.83	18.26

[a] Measured by CV, RDV and DC polarography in acetonitrile and recalculated.[34] [b] Position of the high- and low-energy CT-bands in dichloromethane. [c] DFT-derived ground-state/vertically excited-state dipole moments (M06/6-31G(df,p).

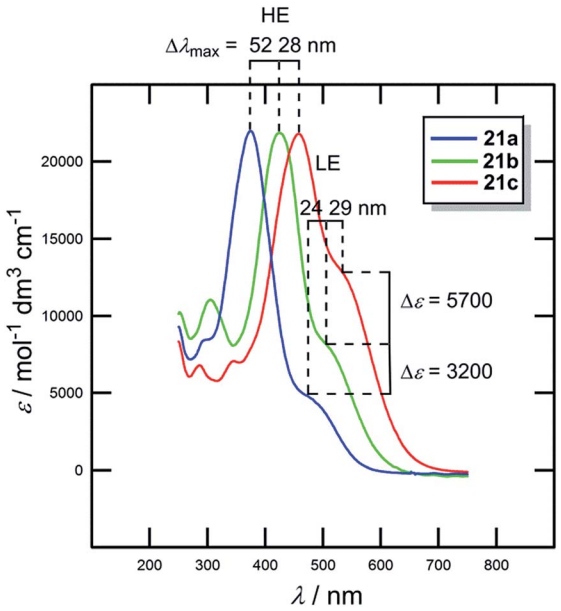

Fig. 16 UV/Vis spectra of chromophores **21a–c** in dichloromethane.

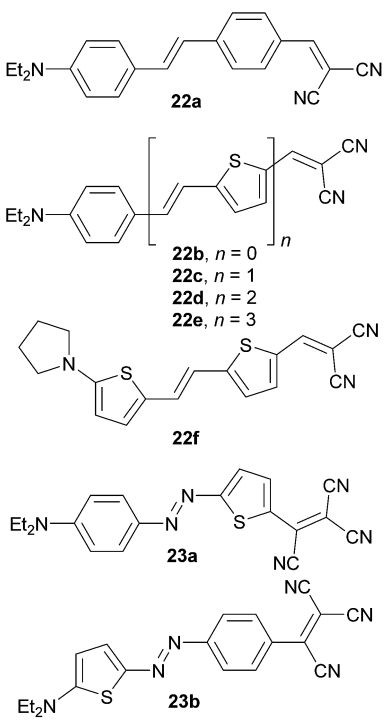

Fig. 17 Thiophene as part of the π-linker.

oligomerization of the vinylenethienylene moiety as in molecules **22b–e**. Both strategies led to significant red shift as well as increased NLO response (Table 11). It is worth mentioning that gradual addition of the vinylenethienylene moiety and observed increase in the NLO response in **22b–e** showed very tight linear correlation with the number of π-electrons (n_π) localized between the *N*,*N*-diethylamino donor and the DCV acceptor (Fig. S3, ESI†). In contrast to benzenoids, no NLO saturation was observed in the NLO phores bearing vinylenethienylene π-linkers. A similar set of push–pull molecules has also been experimentally and theoretically investigated by Wong *et al.*[56] with the same outcome.

In 2004, Moylan *et al.*[57] have reported on two isomeric chromophores **23a–b** (Fig. 17). The effect of the thiophene position within a D–π–A molecule has been studied. It was found that the thiophene on the donor side as in **23b** produces a larger dipole moment; however, the isomer **23a** with thiophene on the acceptor side showed a higher SHG response and has a higher figure of merit for NLO device applications (Table 11).

Raposo *et al.*[58] have investigated structure–property relationships in push–pull oligothiophenes **24a–c** both experimentally and theoretically (Fig. 18). The property tuning has been achieved by gradual elongation of the central oligothiophene scaffold end-capped with the PIT donor and the DCV acceptor. In contrast to the steady bathochromic shift seen in vinylenethienylene chromophores **22b–e** (Table 11), the longest-wavelength absorption maxima in **24a–c** showed the maxima for terthiophene **24b** (λ_{max} = 569 nm, Fig. 18). Push–pull chromophore **24b** showed the NLO response ($\mu\beta$) of 1150 × 10^{-48} esu, which is less than half of that measured for the extended

Table 11 Thiophene-derived D–π–A molecules **22** and **23**

Comp.	μ_{gs} [D]	$\Delta\mu$ [D]	λ_{max} [nm (eV)]	NLO
22a	—	—	468(2.65)[a]	1100[b]
22b	—	—	419(2.96)[a]	300[b]
22c	—	—	513(2.42)[a]	1300[b]
22d	—	—	547(2.27)[a]	2300[b]
22e	—	—	556(2.23)[a]	3800[b]
22f	—	—	584(2.12)[a]	2600[b]
23a	10.8[c]	7.4[d]	719(1.72)[c]	867[e]
23b	12.2[c]	7.0[d]	708(1.75)[c]	686[e]

[a] Measured in dioxane. [b] $\mu\beta_0$ product measured by EFISH experiment (1907 nm) in dioxane [10^{-48} esu]. [c] Measured in chloroform. [d] Difference between the experimentally obtained ground-state and calculated excite-state dipole moments. [e] β_{SHG} measured by EFISH experiment (1907 nm) in chloroform [10^{-30} esu].

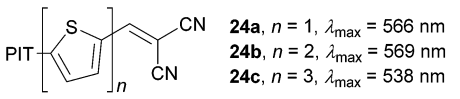

Fig. 18 PIT-oligothiophene-DCV chromophores (λ_{max} in chloroform).

analogous **22f** (2600×10^{-48} esu, Table 11).[59] Hence, planarization of the oligothiophene backbone by an additional olefinic unit plays a very crucial role in tuning the (non)linear optical properties.

Auxiliary donor–acceptor effects of (hetero)cyclic rings incorporated into the π-linker were theoretically studied by Ratner *et al.*[60] The NLO responses were studied in terms of electron excessivity/deficiency of the appended (hetero)ring as well as its aromaticity. Two model D–π–A patterns were investigated in which the NH_2 donor and the NO_2 acceptor were connected to the five-membered electron rich (hetero)cycle and the phenyl ring (**25a–f**) and *vice versa* (**26a–f**, Fig. 19). The calculated properties summarized in Table 12 allow us to distinguish the electron density effects and aromaticity. Whereas the most bathochromically shifted λ_{max} (588 nm) and largest NLO response (237.8×10^{-30} esu) were calculated for **25b**, with the NH_2 donor appended to the electron rich cyclopentadienyl (Cp), the least electron excessive/most aromatic thiophene (**25f**) showed a hypsochromically shifted CT-band (402 nm) and weak NLO response (43.9×10^{-30} esu). On the other hand, the most electron excessive Cp ring in **26b** showed a strongly hypsochromically shifted CT-band (440 nm) and extremely small NLO coefficient (14.7×10^{-30} esu). The largest β value (45.0×10^{-30} esu) within series **26** has been calculated for compound **26f** bearing the aromatic thiophene. Hence, the arrangement of the electron donors and acceptors around the π-conjugated backbone must be well considered when designing a push–pull molecule. Similar relations can be concluded also from the theoretical work of Chandrasekhar *et al.*[61] Namely, the NLO response of a D–π–A molecule depends strongly not only on the nature but also on the location of the heterocyclic ring within the π-linker. For example, a better NLO response can be achieved by placing the electron excessive pyrrole ring close to the D part. The position of a furane unit has a diminished effect, while the aromatic thiophene ring placed close to the A part leads to an enhanced β coefficient.

The length, composition and arrangement of the π-linker play a crucial role, not only for the NLO phores. Since the first Ru-sensitized DSSC reported by Grätzel in 1991,[62] push–pull molecules have also found wide applications as pure (non-Ru) organic photosensitizers (donors). More recently, it has also been realized that optical properties, HOMO/LUMO gap, chemical/thermal stability and energy conversion efficiencies of a DSSC can efficiently be affected by alternation of the π-linker.[63]

A series of thienylene-derived π-conjugated molecules, **27a–e**, which feature a *N*,*N*-diphenylamino donor and cyanoacrylic acid acceptor, and a systematically extended π-linker, has been synthesized by Hagfeldt *et al.* (Fig. 20).[64] A systematic extension and planarization of the π-conjugated path as in the series **27a** → **27b** → **27d** → **27c** → **27e** led to gradual decrease of the HOMO/LUMO energies as well as to bathochromic shift of the longest-wavelength absorption maxima up to 463 nm (Table 13). However, the highest performance has been measured for the DSSC based on **27d** ($\eta = 3.08\%$) The longer

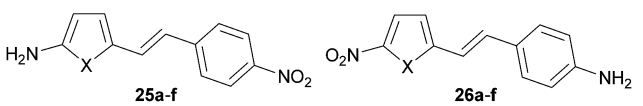

Fig. 19 Two D–π–A patterns in molecules **25** and **26**.

Table 12 Calculated[a] properties of isomeric molecules **25** and **26**

Comp.	X	$\Delta\mu$ [D]	λ_{max} [nm (eV)]	β^b [10^{-30} esu]
25a/26a	CH_2	14.2/11.1	414(3.00)/426(2.91)	51.5/37.4
25b/26b	CH^-	12.2/3.8	588(2.11)/440(2.82)	237.8/14.7
25c/26c	NH	15.6/10.5	418(2.97)/417(2.97)	55.7/33.5
25d/26d	O	13.7/10.7	410(3.02)/424(2.92)	46.6/37.5
25e/26e	PH	15.0/8.4	402(3.08)/434(2.86)	45.9/39.2
25f/26f	S	14.0/10.7	402(3.08)/424(2.92)	43.9/45.0
25d/26d	S	14.0/10.7	402(3.08)/424(2.92)	43.9/45.0

[a] The calculations were carried out using INDO/1 semiempirical Hamiltonian. [b] For optimized geometries.

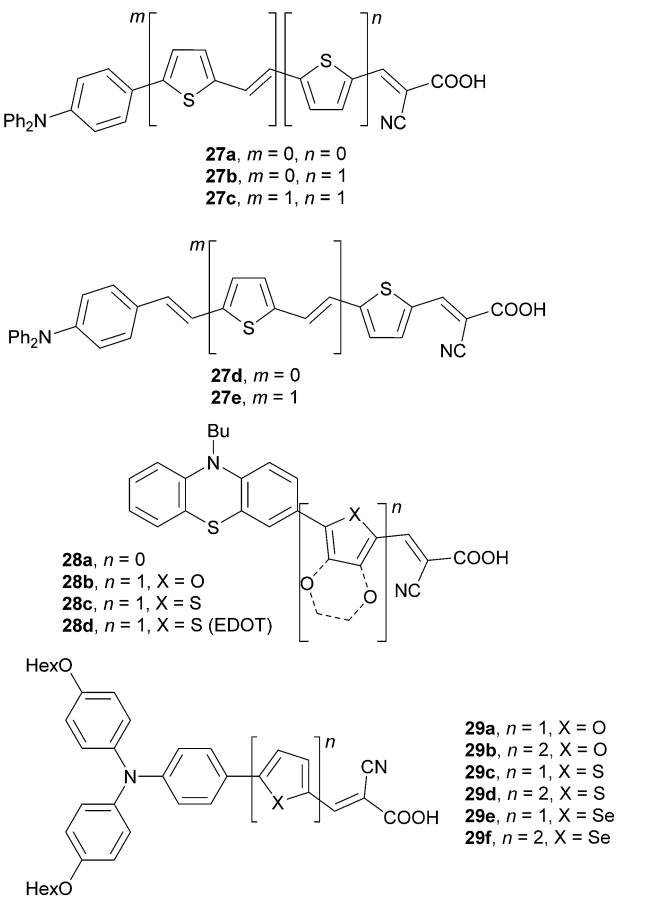

Fig. 20 Push–pull sensitizers **27–29** with various π-linkers.

Table 13 Electronic properties of sensitizers **27**, **28** and **29**

Comp.	$E_{ox,1}$ [V]	$E_{0\text{-}0}$ [eV]	E_{LUMO} [V]	λ^{A}_{max} [nm (eV)]	λ^{E}_{max} [nm (eV)]	η^{DSSC} [%]
27a	1.37[a]	2.90[b]	−1.53[c]	373(3.32)[d]	509(2.44)[d]	1.55
27b	1.21[a]	2.64[b]	−1.43[c]	404(3.07)[d]	548(2.26)[d]	2.75
27c	1.07[a]	2.38[b]	−1.32[c]	445(2.79)[d]	621(2.00)[d]	2.73
27d	1.13[a]	2.48[b]	−1.36[c]	427(2.90)[d]	594(2.09)[d]	3.08
27e	1.01[a]	2.35[b]	−1.34[c]	463(2.68)[d]	644(1.93)[d]	1.70
28a	1.10[e]	2.37[f]	−1.27[c]	452(2.74)[g]	592(2.09)[g]	5.29
28b	0.78[e]	2.26[f]	−1.48[c]	442(2.81)[g]	641(1.93)[g]	6.58
28c	0.89[e]	2.24[f]	−1.35[c]	448(2.77)[g]	634(1.96)[g]	6.32
28d	0.87[e]	2.20[f]	−1.33[c]	466(2.66)[g]	646(1.92)[g]	6.09
29a	−3.35[h]	1.74[h]	−5.09[h]	506(2.45)[i]	689(1.80)[i]	7.17
29b	−3.41[h]	1.62[h]	−5.03[h]	522(2.38)[i]	716(1.73)[i]	7.27
29c	−3.42[h]	1.67[h]	−5.09[h]	514(2.41)[i]	715(1.73)[i]	6.88
29d	−3.48[h]	1.57[h]	−5.05[h]	523(2.37)[i]	723(1.71)[i]	7.67
29e	−3.43[h]	1.66[h]	−5.09[h]	525(2.36)[i]	720(1.72)[i]	7.15
29f	−3.53[h]	1.53[h]	−5.06[h]	549(2.26)[i]	772(1.61)[i]	7.77

[a] Measured by DVP in acetonitrile *vs.* NHE (Fc/Fc^{+}). [b] Transition energy estimated from the intersection of the normalized absorption and emission spectra. [c] $E_{LUMO} = E_{ox,1} + E_{0\text{-}0}$. [d] Absorption and emission maxima measured in acetonitrile. [e] Measured by CV in DMF *vs.* NHE (Fc/Fc^{+}). [f] Estimated from the onset wavelength of the absorption spectra. [g] Absorption and emission maxima measured in dichloromethane. [h] HOMO and LUMO energies and HOMO–LUMO gaps measured by ultramicroelectrode square-wave voltammetry (*vs.* vacuum). [i] Absorption and emission maxima measured in chloroform.

π-linkers as in **27c** or **27e** give increased spectral response (broad IPCEs) but also show pronounced losses (recombination of the electrons to the triiodide).

Phenothiazine dyes **28a–d** were investigated by Kim *et al.* and Hagfeldt *et al.* (Fig. 20).[65] The π-linker has been tailored by incorporation of furan, thiophene and 3,4-ethylenedioxythiophene (EDOT) units. Taking dye **28a** as a standard, the phenothiazine donor linked to a cyanoacrylic acid acceptor through the aforementioned three π-linkers resulted in a small band gap and red-shifted absorption. Sensitizer **28b**, featuring furan within the π-system, showed the highest solar energy-to-electricity conversion efficiency $\eta = 6.58\%$, which is 24% higher than that achieved for **28a**. DSSC based on chromophores **28c/d** with thiophene and electron excessive EDOT showed lower efficiencies and overall performance.

Wang *et al.* have studied the effect of five-membered heteroaromates such as (bi)furan, (bi)thiophene and (bi)selenophene incorporated into the backbone of push–pull dyes **29a–f** on the DSSC performance (Fig. 20).[66] The data in Table 13 nicely demonstrates the impact of the extension and heteroatom replacement within the π-linker on the electrochemical HOMO–LUMO gap and optical properties, as well as the DSSC efficiencies. In accordance with the previous work of Hagfeldt and Kim, dyes featuring furan as part of the π-linker generally showed higher efficiencies than those with thiophene (compare for instance pairs of chromophores **29a**/**29c** and **29b**/**29d**, Table 13). Selenophene showed even better performance than furan (*e.g.* **29e/f** *vs.* **29a/b**). Sensitizers **29b**, **29d** and **29f** with extended π-linkers comprising two consecutive heterocyclic units ($n = 2$) performed generally better in DSSCs than the analogous **29a**, **29c** and **29e** (Table 13). In contrast to the application of push–pull molecules as NLO phores, their performance in DSSCs is less predictable. However, push–pull molecules bearing furan as a part of the π-system seem to be more promising compared to the thiophene analogues.

5. Proaromatic π-systems

Electronic polarization, arising from an applied electric field, of push–pull molecules bearing a ground-state aromatic π-linker (*e.g.* 4-nitroaniline, Fig. 1), is impeded by the concomitant loss of the resonance stabilization. Hence, the effective D–A coupling (ICT process) of a given donor/acceptor pair is suppressed, and formation of the quinoid/zwitterionic structure is rather disfavoured. As a consequence, such molecules generally deliver weak NLO responses. In 1991, Marder *et al.* came up with a new approach for optimizing the hyperpolarizability of π-conjugated molecules.[67] This concept, later named as proaromatic π-linkers/spacers, has recently gained considerable attention as an important tool to achieve property tuning in D–π–A\D–Q–A systems. Marder has originally demonstrated the impact of such structural changes on *N*,*N*-dimethylaminonitrostilbene **30** (DANS, Fig. 21) *vs.* *N*,*N*-dimethylaminoindoaniline **31** (DIA, Fig. 21).

Considering DANS as a standard NLO dye,[68] the absorption maxima and β_0 coefficient of DIA were significantly red-shifted and almost two times higher, respectively. With the same DMA donors, this effect must be attributed to the proaromatic (quinoid) indoaniline acceptor, which gains aromaticity upon

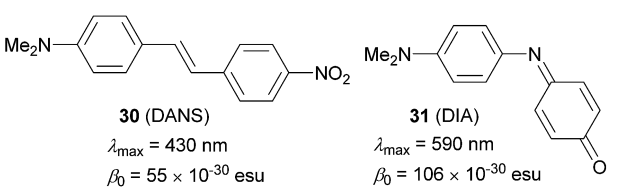

Fig. 21 Marder's demonstration of (pro)aromatic spacers in DANS and DIA (data measured in chloroform).

excitation (reversal to the resonance forms shown in Fig. 1). In fact, either the acceptor/donor or both quinoid parts may be present in the currently known proaromatic push–pull molecules.

Diederich[69] *et al.* have shown tripodal push–pull molecules **32a–d** bearing a proaromatic withdrawing moiety structurally similar to **31**. However, due to the presence of an additional DCV unit, it represents an even stronger electron acceptor (Fig. 22).[69] Molecule **32a** has also been reported by Oda.[70]

In contrast to **32a–b**, molecules **32c–d** were oxidized (quinoid) only partially. Further expansion of the benzoquinone ring has been demonstrated by the synthesis of the radiaannulene quinoid molecule **33**. Evidence of proaromaticity has been presented in terms of structural, spectroscopic, electrochemical and computed data (Table 14). When comparing a pair of fully/partially quinoid chromophores **32a**/**32c** the HOMO–LUMO gap decreased from 1.83 to 1.47 eV and the absorption maximum was red-shifted by 170 nm. Extension of the π-system by two additional acetylenic spacers (**32c** → **32d**) had a diminished effect, whereas insertion of an additional benzoquinone ring as in **32b** shifted the first oxidation potential to negative values; the HOMO–LUMO gap was reduced to 0.91 eV and the longest-wavelength absorption maximum reached the NIR region (845 nm). This series of molecules nicely demonstrates how powerful tuning through proaromatic spacers can be ($\Delta E_g = 0.92$ eV, $\Delta\lambda_{max} = 317$ nm). Moreover, the observed negative solvatochromism further confirms the strong charge-separation in the ground state. Radiaannulene **33** showed electrochemical and optical properties at the level of chromophores **32a**/**32d**.

Currently well-elaborated proaromatic electron donating groups comprise mostly 4*H*-pyran-4-ylidene,[12] pyridine-4-ylidene[71,72] and 1,3-dithiol-2-ylidene (dithiafulvene)[73,74] (Fig. 23).

4*H*-Pyran-4-ylidene and its application as an electron donor has been extensively studied by Garín *et al.*[12a,b] For instance, they have studied push–pull molecules **34a–d** (Fig. 24) end-capped with a proaromatic donor and tricyanofuran (TCF) acceptor with systematically extended polyenic central spacer. Later on, the pyran moiety has also been used as a central spacer and the linear chromophore arrangement as in **35a–b** has been completed with the V-shaped molecule **36** (Fig. 24). The fundamental optoelectronic properties and optical nonlinearities of these molecules were further investigated (Table 15). Gradual extension of the polyenic central spacer in

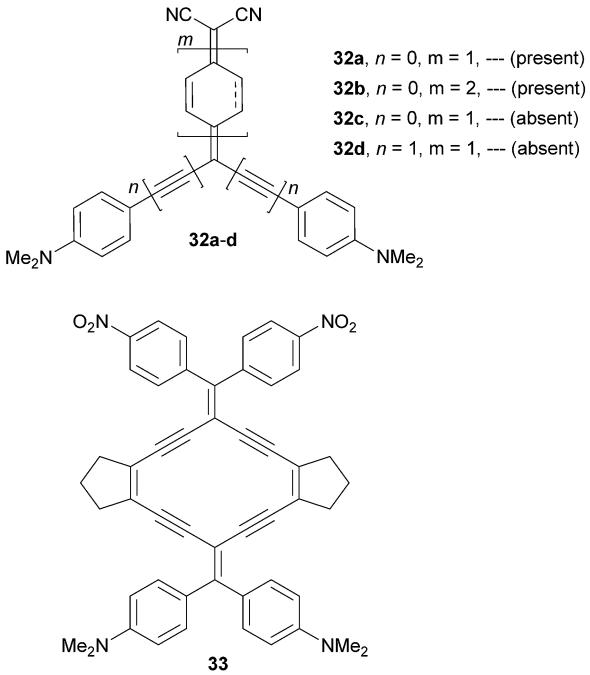

Fig. 22 Proaromatic chromophores**32a–d** and radiaannulene **33**.

Table 14 Electrochemical and optical data for chromophores **32** and **33**

Comp.	$E_{ox,1}$[a] [V]	$E_{red,1}$[a] [V]	E_g [eV]	λ_{max}[b] [nm (eV)]
32a	0.17	−1.30	1.47	698(1.78)
32b	−0.18	−1.09	0.91	845(1.47)
32c	0.48	−1.35	1.83	528(2.35)
32d	0.33	−1.45	1.78	531(2.33)
33	0.16	−1.38	1.54	586(2.12)

[a] Measured in dichloromethane, *vs.* Fc^+/Fc. [b] Measured in dichloromethane.

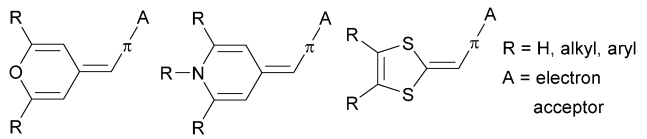

Fig. 23 Proaromatic donor moieties.

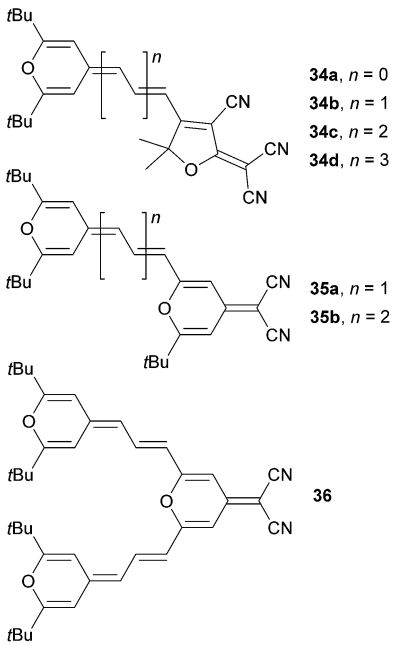

Fig. 24 4*H*-Pyran-4-ylidene proaromatic donor.

34a–d reduced the HOMO–LUMO gap and red-shifted the λ_{max} up to 688 nm. The NLO response ($\mu\beta_0$) increased dramatically from 90 (**34a**) to 3110 × 10^{-48} esu (**34d**). Similar trends can be seen in molecules **35a–b**; however when going from **35a** to **36** (linear *vs.* V-shaped arrangement), the second π-conjugated branch in **36** had a small influence on the optoelectronic properties (Table 15).

Dipolar and quadrupolar organic dyes with a diphenylmethylenepyran donor were also studied by Achelle *et al.* (Fig. 25 and Table 16).[12d] Linear molecules **37a–d** were synthesized by Wittig olefination, Sonogashira cross-coupling and eventually Knoevenagel condensation. Bismethylenepyran derivative **38** was prepared by oxidative dimerization of **37a** in the presence of a $I_2/Na_2S_2O_3$ oxidation/reduction system. In contrast to the extension of the π-system as in **34a–d** (Table 15), variation of the peripheral acceptor (CN → NO_2 → CF_3 → DCV) did not affect the electrochemically measured first oxidation and reduction potentials. This can be explained by the formation of a pyrylium radical $\mathbf{34}^{+\bullet}$, which undergoes facile electrochemical dimerization to bispyrylium compounds similar to $\mathbf{38}^{2+}$. The longest wavelength absorption maxima of **37a–d** and **38** shift slightly bathochromically with increased electron withdrawing ability of the appended A-groups. The highest NLO coefficient has been measured for DCV-substituted derivative **37d** ($\mu\beta$ = 1150 × 10^{-48} esu); quadrupolar derivative **38** showed average NLO performance.

4-Methylene chalcogenapyrans as proaromatic donors were also utilized in the synthesis of push–pull Fischer type carbene complexes **39a–c** (Fig. 26).[12c] Depending on the chalcogen atom involved, these molecules exhibited (non)linear optical properties with λ_{max} = 594–613 nm and $\mu\beta$ = 1219–2348 × 10^{-48} esu, respectively. Thiopyran-based molecule **39b** delivered the strongest NLO response.

A series of molecules **40a–c** was prepared by Woolhouse *et al.* (Fig. 27, Table 17).[71] In these molecules, proaromatic pyridine-4-ylidene and TCF act as electron donor and acceptor, respectively. When comparing **40a–c** with isolobal **34a–c** (Fig. 24), the later series showed a more rapid bathochromic shift and a larger increase in the NLO coefficient, accompanied by the extension of the polyene spacer.

Table 15 Electrochemical and (nonlinear) optical properties of **34–36**

Comp.	$E_{ox,1}$[a] [V]	$E_{red,1}$[a] [V]	E_g [eV]	λ_{max}[b] [nm (eV)]	$\mu\beta_0$[c] [10^{-48} esu]
34a	1.32	−1.10	2.42	513(2.42)	90
34b	1.00	−0.83	1.83	592(2.09)	310
34c	0.68	−0.77	1.45	675(1.84)	1520
34d	0.51	−0.69	1.20	688(1.80)	3110
35a	0.76	−1.18	1.94	587(2.11)	652
35b	0.59	−1.21	1.80	602(2.06)	1370
36	0.72	−1.12	1.84	633(1.96)	1500[d]

[a] Measured in dichloromethane, *vs.* Ag/AgCl. [b] Measured in dichloromethane. [c] EFISH experiment at 1907 nm (dichloromethane). [d] $\mu\beta$ value.

Table 16 Electrochemical and (nonlinear) optical properties of **37–38**

Comp.	$E_{ox,1}$[a] [V]	$E_{red,1}$[a] [V]	λ_{max}[c] [nm (eV)]	$\mu\beta$[d] [10^{-48} esu]
37a	0.31	−0.87[b]	414(3.00)	350
37b	0.32	−0.86[b]	432(2.87)	200
37c	0.32	−0.89[b]	403(3.08)	700
37d	0.31	−0.85[b]	463(2.68)	1150
38	−0.16	—	453sh(2.74)	830

[a] Measured in dichloromethane, *vs.* Fc^+/Fc. [b] Represent reduction of the bispyrylium dication. [c] Measured in dichloromethane. [d] EFISH experiment at 1907 nm (chloroform).

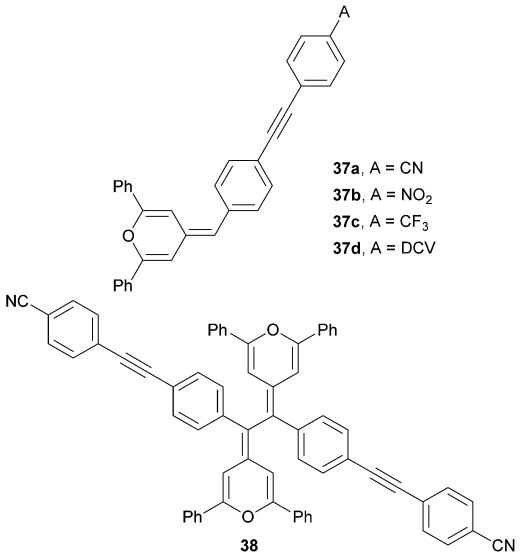

Fig. 25 Dipolar and quadrupolar NLO phores bearing diphenylmethylenepyran donor(s).

Fig. 26 Chalogenapyrans in push–pull Fisher type carbene complexes.

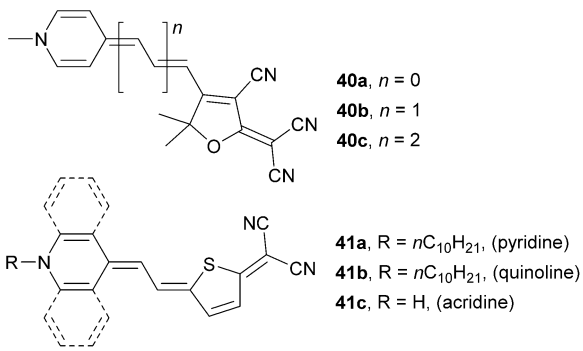

Fig. 27 Pyridine-4-ylidene and related proaromatic donors.

Table 17 (Non)linear optical properties of **40–41**

Comp.	λ_{max} [nm (eV)]	β_0 [10^{-30} esu]
40a	570(2.17)[a]	125[b]
40b	600(2.07)[a]	360[b]
40c	615(2.02)[a]	500[b]
41a	619(2.00)[c]	-92 ± 15[d]
41b	714(1.74)[c]	66 ± 18[d]
41c	787(1.58)[c]	338 ± 14[d]

[a] Measured in DMF. [b] HRS experiment in DMSO. [c] Measured in DMSO. [d] Deduced from the electro-optical absorption and UV/Vis spectra using a two-level model, in 10^{-50} CV^{-2} m^3 (dioxane).

Table 18 Selected properties of dithiafulvene-derived molecules **42–43**

Comp.	$E_{ox,1}$[a] [V]	$E_{red,1}$[a] [V]	E_g [eV]	λ_{max}[b] [nm (eV)]	$\mu\beta_0$[c] [10^{-48} esu]
42a	1.25	−0.85	2.10	590(2.10)	135
42b	0.85	−0.68	1.53	688(1.80)	935
42c	0.68	−0.57	1.25	715(1.73)	3640
43a	0.94	−0.78	1.72	653(1.90)	609
43b	0.75	−0.72	1.47	732(1.69)	1938
43c	0.61	−0.64	1.25	835sh(1.49)	6173

[a] Measured in dichloromethane, *vs.* Ag/AgCl. [b] Measured in dichloromethane. [c] EFISH experiment at 1907 nm (dichloromethane).

Abbotto *et al.* focused on the synthesis and thorough structure–property relationships study on molecules **41a–c** bearing pyridine-4-ylidene donor gradually annulated with one or two benzene rings (quinoline and acridine derivatives, Fig. 27).[72] As can be seen from the data given in Table 17, fusion of the benzene(s) to the pyridine-4-ylidine donor red-shifts the absorption maxima and the NLO coefficient to positive values. It was concluded that **41a–c** are highly polarizable molecules, primarily zwitterionic and their NLO response strongly depends on the environment (solvent/matrix). In general, the NLO activity estimation should be carried out in various media to avoid unfortunate choice of solvent as dictated by instrumental availability and solubility properties.

Garín *et al.* have also investigated proaromatic dithiafulvene donor moiety attached either on 1,1,3-tricyano-2-phenylpropene (**42**) or TCF (**43**) acceptors (Fig. 28).[73,74]

As expected, the HOMO–LUMO gap was narrowed, the λ_{max} was shifted bathochromically and the NLO coefficient was raised with extension of the central olefinic backbone (Table 18). A comparison of molecules **34c** ($E_g = 1.45$ eV, $\lambda_{max} = 1.84$ eV and $\mu\beta_0 = 1520 \times 10^{-48}$ esu), **40c** ($\lambda_{max} = 2.02$ eV and $\mu\beta_0 = 8900 \times 10^{-48}$ esu) and **43b** ($E_g = 1.47$ eV, $\lambda_{max} = 1.69$ eV and $\mu\beta_0 = 1938 \times 10^{-48}$ esu) bearing TCF acceptor, the same polyenic spacer ($n = 2$) and differ only in the attached proaromatic electron donor seems to be reasonable at this point. Molecules **34c** and **43b** having 4*H*-pyran-4-ylidene and dithiafulvene donors showed very similar electrochemical and optical gaps. The optical gap of pyridine-4-ylidine-substituted chromophore **40c** is higher by more than 0.2 eV but this molecule delivered 4–5 times stronger NLO response than analogues **34c** and **43b**. However, an artificial enrichment of this value due to the used calculated dipole moment μ cannot be excluded.

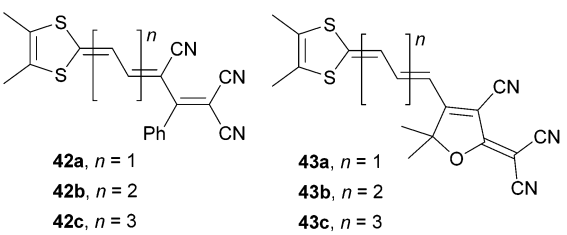

Fig. 28 Dithiafulvene proaromatic donors in push–pull molecules.

Anyway, very similar trends can be seen in the comparative study carried out by Garín *et al.*[75] Three analogous molecules **44**, **45** and **46** (Fig. 29) bearing the aforementioned proaromatic donors were synthesized and investigated. Despite its highest electrochemical and optical gaps, the NLO performance of pyridine-4-ylidene-substituted derivative **45** is 4 to 6-times higher than that of **44** and **46**. Hence, pyridine-4-ylidenene proaromatic donor seems to be the most efficient one when designing new NLO phore with high nonlinearities.

A combination of proaromatic donor and acceptor parts would render the most powerful D–Q–A chromophores. The first synthesis of such fully quinoid push–pull molecules **47** carried out by Gompper *et al.* can be dated back to 1966–1968 (Fig. 30).[76] In late 90's, extended molecules **48–51** were prepared and spectrally/electrochemically investigated by Otsubo[77,78] and Bryce[79] (Fig. 30). As can be seen, extension of the parent molecule **47** by an additional benzoquinone ring (**48**) shifted the absorption maxima by 400 nm. Likewise, whereas chalcogen exchange in **49** did not significantly affect the optical properties, extension of the π-system by one additional thienylene unit resulted in chromophores **50a–b** with the absorption maxima exceeding 700 nm. Property tuning in anthraquinone-derived molecules **51a** has been accomplished by attaching stronger DCV and N–CN acceptors. This provided chromophores **51b–c**

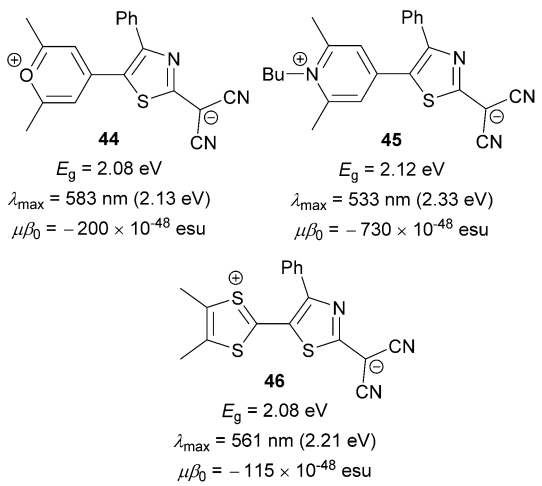

Fig. 29 Performance of pyran-4-ylidene, pyridine-4-ylidene and dithiafulvene proaromatic donors in push–pull molecules.

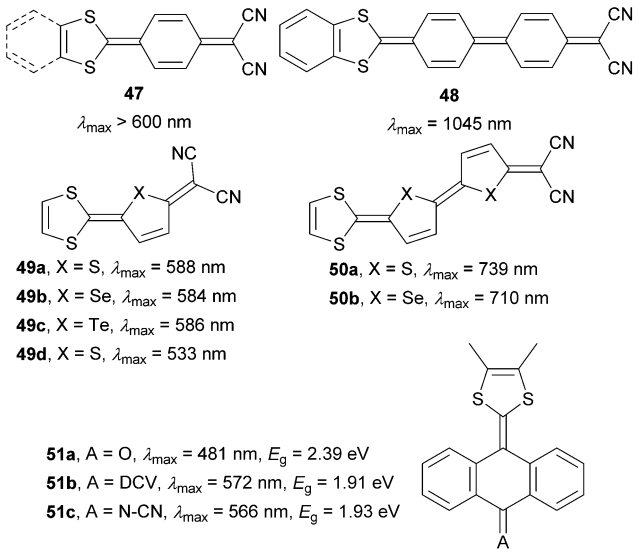

Fig. 30 Fully quinoid dyes **47–51**.

with narrowed band gaps and bathochromically shifted CT-bands.

Novel doubly proaromatic NLO phores **52–57** were investigated by Garín *et al.* (Fig. 31).[80–82] In molecules **52** and **53** is the 4,5-dimethyldithiafulvene donor linked *via* expanded olefinic bridge to proaromatic thiobarbituric acid. Extension of the π-system lowered the HOMO–LUMO gap, red-shifted the CT-band and increased the NLO coefficient $\mu\beta_0$ (compare pairs of chromophores **52a**/**52b** or **53a**/**53c**, Table 19). Although well polarizable, polyenic spacers often suffer from thermal, chemical and conformational instability. This is also the reason why molecule **53b** was not isolated. However, a comparison of **52b** and **53a** possessing the same number of double bonds (π-electrons) and conformationally (un)locked π-system, reveals that the latter (isophorone-locked) features narrowed band gap and two-times higher NLO response. Very similar conclusions

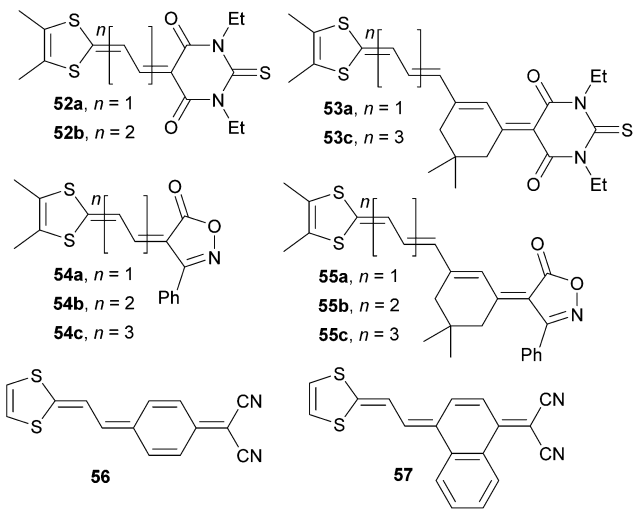

Fig. 31 Novel doubly proaromatic NLO phores.

Table 19 Properties of doubly proaromatic NLO phores **52–57**

Comp.	$E_{ox,1}$[a] [V]	$E_{red,1}$[a] [V]	E_g [eV]	λ_{max}[b] [nm (eV)]	$\mu\beta_0$[c] [10^{-48} esu]
52a	1.16	−1.00	2.16	558(2.22)	60
52b	0.87	−0.85	1.72	642(1.93)	525
53a	0.65	−0.81	1.46	638(1.94)	1135
53c	0.48	−0.77	1.25	638(1.94)	1350
54a	1.06	−1.12	2.18	547(2.27)	153
54b	0.77	−0.93	1.70	621sh(2.00)	565
54c	0.59	−0.82	1.41	633(1.96)	1091
55a	0.59	−0.95	1.50	606(2.05)	1475
55b	0.50	−0.91	1.41	614(2.02)	2229
55c	0.43	−0.86	1.29	622(1.99)	2843
56	0.63	−0.64	1.27	652(1.90)	−667
57	0.74	−0.63	1.37	672(1.85)	115

[a] Measured in dichloromethane, *vs.* Ag/AgCl. [b] Measured in dichloromethane. [c] EFISH experiment at 1907 nm (dichloromethane).

can also be evaluated from the series **54a–c** and **55a–c** in which the six-membered thiobarbituric acid acceptor was replaced by five-membered isoxazolone. A comparison across both series reveals similar electrochemical gaps, slightly hypsochromically shifted CT-bands for isoxazolone-substituted molecules **54** and **55** (an additional blue-shift observed for isophorone-bridged molecules **55a–c** is also noticeable) and generally higher nonlinearities measured for isoxazolone derivatives **54** and **55** (compare for instance pair of chromophores **52b**/**54b** and **53c**/**55c**, Table 19). Effect of benzo-annulation was demonstrated on molecules **56** and **57**. Likewise to observation on annulation at pyridine-4-ylidene donor made by Abbotto (**41a–c**, Fig. 27 and Table 17), chromophore **57** showed bathochromically shifted CT-band and positive value of $\mu\beta_0$ (Table 19). This further implies that NLO phore **56** possesses considerably zwitterionic (quinoid) ground state which was also evidenced by X-ray analysis and DFT calculations.

6. Tuning through the acceptor

The property tuning in D–π–A molecules can also be accomplished *via* alternation, addition and position of the acceptor part. The A-part is most frequently represented by functional groups with negative resonance and inductive effects such as cyano, nitro and carbonyl as well as their combinations.

For example, a variation of electron withdrawing groups on the amino-substituted styrenes **58a–c** and diphenylacetylenes **59a–f** has been performed by Cheng *et al.* (Fig. 32, Table 20).[37a,39b] From the data given in Table 20 we can deduce that nitro and cyano groups induce the most efficient ICT in the push–pull molecules and thus red-shift the absorption edge and increase the first-order hyperpolarizability. The formyl group also seems to be very powerful, however this moiety is chemically much more reactive and therefore less commonly used. Moderate polarizations/nonlinearities were observed for molecules **59a–59d** bearing acyl, benzoyl methoxycarbonyl and methylsulfonyl groups.

Vivas *et al.* carried out a comprehensive structure–property relationships study on non-centrosymmetric two-photon

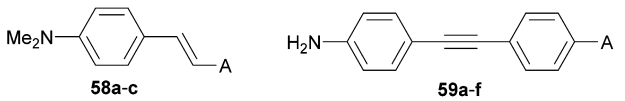

Fig. 32 Acceptor variation on styrene and diphenylacetylene D–π–A systems.

Table 20 Styrenes **58a–c** and diphenylacetylenes **59a–f**

Comp.	A	$\mu_g/\Delta\mu^a$ [10^{-18} esu]	$\lambda_{max}{}^b$ [nm (eV)]	β/γ^c [$10^{-30/36}$ esu]
58a	CN	6.0/—	364(3.41)	23/29
58b	CHO	5.6/—	384(3.23)	30/63
58c	NO_2	6.5/—	438(2.83)	50/—
59a	$COCH_3$	3.3/12.6	336(3.69)	12/—
59b	COPh	3.7/9.9	352(3.52)	19/—
59c	CO_2Me	3.8/10.6	337(3.68)	15/—
59d	SO_2Me	6.5/6.6	338(3.67)	13/—
59e	CN	5.2/4.3	343(3.62)	20/—
59f	NO_2	5.5/9.5	379(3.27)	24/—

[a] Ground state dipole moments and its change upon excitation (solvatochromism of the CT-band). [b] Measured in chloroform. [c] First- and second-order hyperpolarizabilities measured by EFISH and THG experiments (1910 nm).

absorbing molecules **60a–f** based on triarylamine (Fig. 33).[83] The property tuning has been accomplished by variation of the acceptor group A appended at one of the aryl rings (Table 21).

On increasing the electron withdrawing capability of A (from **60b** to **60f**, Table 21), the absorption and emission maxima shift bathochromically, and the changes in dipole moment and degree of ICT increase from 9–13.5 D and 34 to 54%, respectively. As expected, the DCV acceptor causes the highest polarization. More importantly, the measured TPA cross-section mimics similar trends with the highest TPA coefficient $\sigma = 125$ GM measured for **60f**.

The aforementioned examples imply that replacing simple electron withdrawing groups (*e.g.* CN or NO_2) with more structurally complex electron accepting moieties (*e.g.* DCV) leads to push–pull molecules with significantly enhanced ICT. In this respect, various (hetero)aromates were utilized, not just as spacers and auxiliary donors (see above), but also as powerful

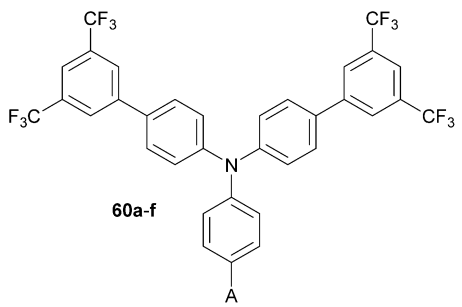

Fig. 33 Various acceptors in non-centrosymmetric two-photon absorber **60**.

electron acceptors. Several examples of property tuning through the acceptor are shown in Fig. 34.

Dimethylanilino-substituted D–π–A fluorescent thiophenes **61a–c** were prepared and investigated by Blanchard-Desce and Raposo.[40b,84] Gradual replacement of the formyl group in **61a** by DCV (**61b**) and *N*,*N*′-diethylthiobarbituric acid (**61c**) acceptors led to bathochromic shift of the longest-wavelength absorption maxima and increased two-photon absorption cross-section, as well as higher thermal stability (Table 22). Moylan *et al.* carried out property tuning through the acceptor in a series of azo NLO phores **62a–c** (Fig. 34).[49] The aromatic 4-nitrophenyl acceptor (**62a**) has been replaced by heteroaromatic 5-nitrothiazole (**62b**) and 6-nitrobenzo[*d*]thiazole (**62c**). These structural changes resulted in chromophores with red-shifted λ_{max}, higher ground-state dipole moments and first-order hyperpolarizabilities β_0 within the range 57–71 $\times$ 10^{-30} esu. Thermal stability of **62a–c** up to/over 300 °C is also noticeable. Thiobarbituric acid, although considered to be a very strong electron acceptor, can be replaced by the even stronger 3-dicyanomethylene-2,3-dihydrobenzo[*d*]thiophene-1,1-dioxide as in **63a–b** (Fig. 34).[40a] Both chromophores showed the same ground-state dipole moments and similar changes upon excitation. However, with the same donor and π-linker as in **63a**, **63b** features a bathochromically shifted CT-band by 106 nm and 1.3-times higher nonlinearity. An interesting comparison of electron acceptors involving benzo[*d*]furan-3-one (**64a**), dicyanovinyl (DCV, **64b**), *N*,*N*′-diethylthiobarbituric acid (**64c**) and 3-(dicyanomethylene) indane-1-one (**64d**) and their impact on (non)linear optical properties has been demonstrated by Roncali *et al.* (Fig. 34).[85] The rigidified bithiophene central spacer end-capped with a DMA donor and gradual replacement of acceptors allowed optical tuning by 176 nm and increased the NLO response by almost 4-times. Hence, 3-(dicyanomethylene)indane-1-one proved to be the strongest donor in this series.

Based on our recent contributions, dicyano-substituted (hetero)aromatic acceptor units based on imidazole, benzene and pyrazine can be compared with barbituric acid here. Y-shaped dicyanoimidazole (DCI),[32] X-shaped dicyanobenzene (DCB)[86] and dicyanopyrazine (DCP),[23] as well as *N*,*N*′-dibutylbarbituric acid (BA)[87] derivatives **2c** and **65–67** saturated by one or two DMA donor(s), can be chosen as model push–pull molecules (Fig. 35). Table 23 and the energy level diagram in Fig. 36 summarize the electrochemical and optical data as well as the measured NLO properties. As expected, the main changes in frontier orbitals are observed in the LUMO while the HOMO remained almost unaltered (E_{HOMO} = 5.27–5.42 eV). When going from five-membered DCI (**2c**) to six-membered DCB (**65**) and DCP (**66**) acceptors, the HOMO–LUMO gap decreases stepwise by roughly 0.3 eV. The lowest gap was measured for DCP and BA derived compounds **66** and **67**. Thus, DCI seems to be the weakest electron acceptor (two cyano groups attached at electron excessive imidazole), DCB behaves as a "standard aromatic acceptor" while replacement of two CH groups by nitrogens as in DCP narrowed the gap by an additional 0.3 eV (two cyano groups attached at the electron poor pyrazine).

One has to take into consideration that DCI is saturated by one DMA donor, whereas DCB and DCP are saturated by two

Table 21 Properties of tripodal molecules **60a–f**

Comp.	A	$\lambda_{max}^{A/E}$ [a] [nm]	Φ_{max}^{E}	$\Delta\mu$ [c] [D]	r_{eff}/r [d] [%]	σ [e] [GM]
60a	H	361/428	0.46[b]	10.5	42	65
60b	CN	347/422	0.24[b]	9.5	34	58
60c	CHO	359/437	0.19[b]	9.0	35	48
60d	NO_2	394/525	0.40[b]	11.5	46	45
60e	CH=C(CN)CO_2Et	426/510	0.13[b]	13.0	54	115
60f	DCV	439/535	0.24[b]	13.5	54	125

[a] Absorption/emission maxima (toluene). [b] *vs.* POPOP ($\Phi = 0.93$ in cyclohexane). [c] Dipole moment changes upon excitation. [d] Degree of the ICT, where $r_{eff} = \Delta\mu/e$ defines the effective charge transfer (e = electron charge) and r is the distance between the amino core (donor) and the first atom of the acceptor (DFT calculation). [e] TPA cross-section measured by Z-scan at 775 nm in toluene [GM].

DMA donors. However, the BA acceptor saturated by one DMA donor provided a similar gap ($E_g = 2.25$ eV) to DCP ($E_g = 2.26$ eV). It should also be mentioned that the DMA units in **2c**, **65** and **66** are connected directly to the DCI, DCB and DCP acceptors with torsion angles 25–42° (see X-ray analyses in Fig. 35), whereas an additional methylene bridge in **67** causes planarization of the π-system (torsion angle about 4°). A significant twist of DMA(s) in **2c**, **65** and **66** is most likely caused by the steric repulsion of the *ortho*-hydrogens and represents an additional barrier to efficient ICT.

The UV/Vis absorption spectra of **2c** and **65–67** are shown in Fig. 37; the longest-wavelength absorption maxima are presented in Table 23. The optical properties mimic the trends seen by electrochemical measurements (E_g) with $\Delta\lambda_{max}$ of 155 nm. DCP- and BA-derived molecules **66** and **67** showed the most red-shifted CT-bands. Moreover, two particular CT-bands were observed for X-shaped molecule **66** and less developed also for **65**. These bands are most likely originated by multiple interactions of each peripheral donor and the particular CN acceptor (Fig. 37). DCP-derivatives also proved to be very efficient and tuneable photoredox catalysts.[23b]

In principle, the withdrawing ability of azo-heterocyclic acceptors can further be improved by quaternization (see for instance molecules **12a–e**, Fig. 7)[41] or chelation by a (transition) metal.[88] Electronic performance of the most frequently used cationic acceptor, pyridinium, can be for instance compared with fused five-membered benzo[*d*]thiazolium, as shown by Coe *et al.* (Fig. 38).[89] Replacing the pyridinium acceptor in chromophoric cations **68** led to **69** with reduced HOMO–LUMO gap, red-shifted CT-band and pronounced NLO response measured by HRS at two laser frequencies (Table 24). Hence, the benzothiazolium ion can be considered as a stronger electron acceptor than the pyridinium ion. Further property tuning in **68–69** has been achieved by extension of the central olefinic spacer, which could also be substituted by thienylene units, as demonstrated by Clays *et al.*[90]

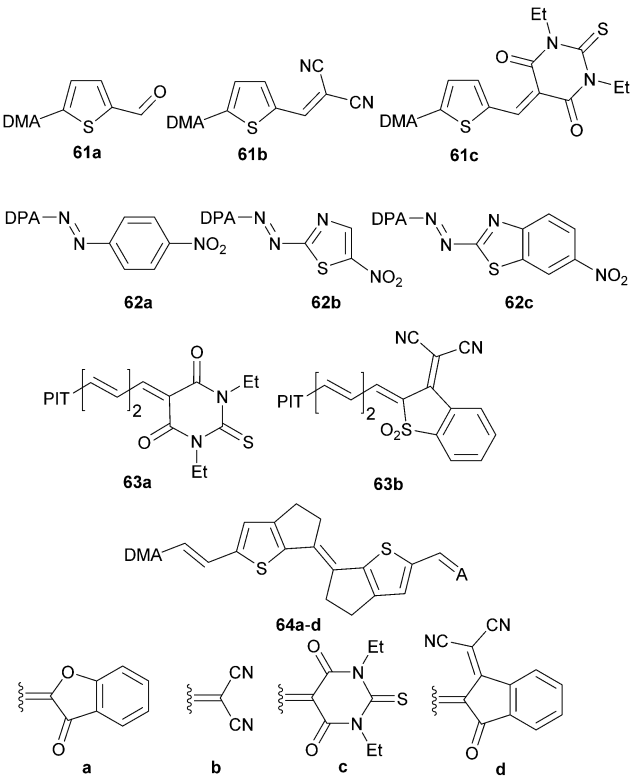

Fig. 34 Property tuning through the acceptor (DMA = 4-(*N*,*N*-dimethylaminophenyl), DPA = 4-(*N*,*N*-diphenylamino)phenyl, PIT = 5-(piperidin-1-yl)thiophene-2-yl).

Table 22 Selected data of chromophores **61–64**

Comp.	$\lambda_{max}^{A/E}$ [nm]	$\mu/\Delta\mu$ [D]	NLO	T_d [°C]
61a	408/507[a]	—/—	124(820)[b]	190[c]
61b	512/609[a]	—/—	176(1050)[b]	209[c]
61c	572/669[a]	—/—	428(1120)[b]	260[c]
62a	486[a]/—	5.9/—	54.3[d]	393
62b	582[a]/—	6.9/—	68.2[d]	295
62c	550[a]/—	7.2/—	71.8[d]	356
63a	619[a]/—	10.4/6.1	55[d]	240
63b	725[a]/—	10.4/7.7	72[d]	268
64a	592[e]/—	—	1500[f]	300
64b	614[e]/—	—	1600[f]	308
64c	682[e]/—	—	4400[f]	235
64d	768[e]/—	—	5680[f]	245

[a] Measured in chloroform. [b] TPA cross-section (wavelength) measured by two-photon excited fluorescence (TPEF) in chloroform, relative to fluorescein [GM]. [c] Melting point. [d] First-order hyperpolarizabilities measured by EFISH experiments (1907 nm) in chloroform. [e] Measured in dichloromethane. [f] $\mu\beta_0$ product measured by EFISH experiments (1907 nm) in chloroform.

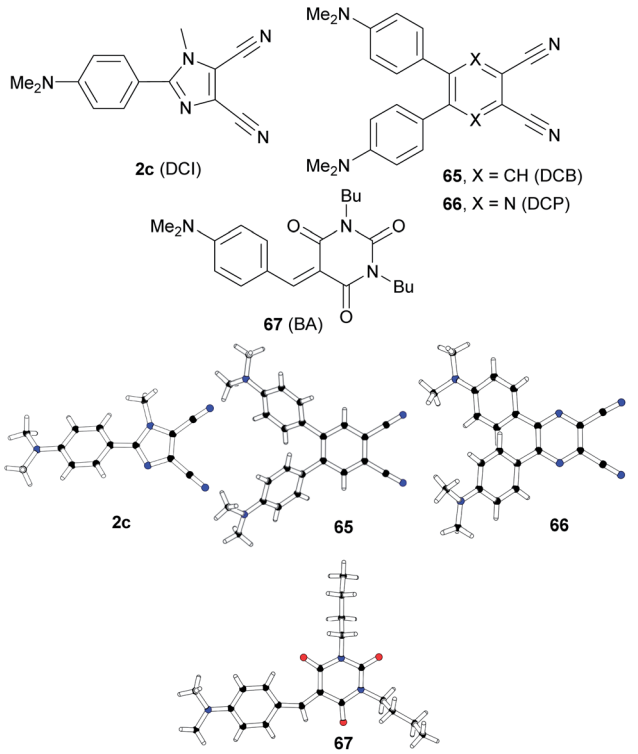

Fig. 35 Structure of DCI, DCB, DCP and BA acceptor units in push–pull molecules **2c** and **65–67**, including their X-ray analyses.

Table 23 Optoelectronic properties of DCI, DCB, DCP and BA derivatives

Comp.	E_{HOMO}[a] [eV]	E_{LUMO}[a] [eV]	E_g [eV]	λ_{max}[b] [nm (eV)]	NLO
2c	−5.36	−2.51	2.85	316(3.92)	19.2[c]
65	−5.27	−2.73	2.54	410(3.02)	0.53[d]
66	−5.37	−3.11	2.26	471(2.63)	—[d]
67	−5.42	−3.17	2.25	462(2.68)	270(36)[e]

[a] Measured by CV, RDV and DC polarography in acetonitrile/DMF and recalculated.[34] [b] Measured in dichloromethane at $c = 10^{-5}$ M. [c] First order hyperpolarizability measured by HRS experiment (1064 nm) in dichloromethane (in 10^{-30} esu). [d] Second-order susceptibility of **65**/**66** incorporated into oligoetheracrylate photopolymer (1064 nm). The signal for **66** was below noise level (in pm V^{-1}). [e] $\mu\beta$ product (β) measured by EFISH experiment (1907 nm) in chloroform (in $10^{-48(30)}$ esu).

Barbituric acid related push–pull derivatives **70–73** were targeted in a brief contribution of Ikeda *et al.* (Fig. 39).[91] In these molecules, the DMA donor was linked to *N*-unsubstituted barbituric acid (**70**), thiobarbituric acid (**71**), hydantoin (**72**) and rhodanine (**73**). When going from barbituric acid to thiobarbituric acid acceptors (**70** → **71**), the measured linear and nonlinear optical properties (λ_{max} and $\mu\beta_0$) were shifted by 30 nm and 520 × 10^{-48} esu, respectively. This enhancement was attributed to the chalcogen effect. On the other hand, contraction of the six-membered BA derivative **70** to the hydantoin derivative **72** resulted in considerable hypsochromic shift and diminished NLO response. Compared to **72**, two sulphur atoms

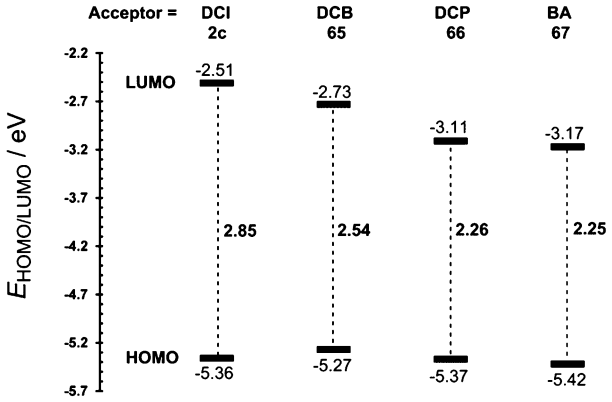

Fig. 36 Energy level diagram showing HOMO/LUMO of **2c** and **65–67**.

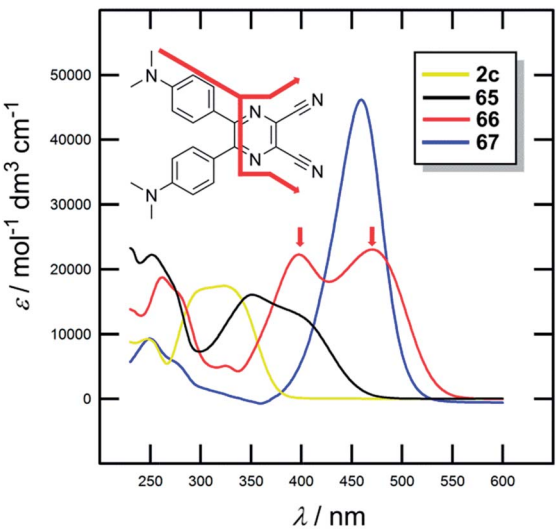

Fig. 37 UV/Vis absorption spectra of **2c** and **65–67**.

in rhodanine derivative **73** shifted the CT-band by 90 nm and renewed the large NLO response ($\mu\beta_0$ = 1050 × 10^{-48} esu). Hence, the ring size and heteroatoms attached on it may play a very crucial role in the overall performance of the given heterocyclic acceptor.

Garín *et al.* have demonstrated property tuning through acceptors on push–pull molecules **74–78** (Fig. 40 and Table 25) comprising a proaromatic pyran-4-ylidene donor and complex acceptor groups such as thiobarbituric acid (**74**), isoxazolone (**75**), phenyl- and amino-substituted tricyanopropene (**76** and **77**) and tricyanofuran (**78**).[12a] The lowest electrochemical gaps were recorded for tricyano-substituted derivatives **76** and **78**, which also reflects their most bathochromically shifted CT-

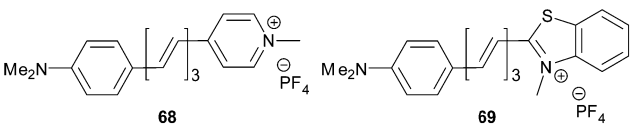

Fig. 38 Cationic chromophores.

Table 24 Electrochemical data and (non)linear optical properties of 68–69

Comp.	$E_{ox,1}$[a] [eV]	$E_{red,1}$[a] [V]	E_g [eV]	λ_{max}[b] [nm (eV)]	β_0[c] [10^{-30} esu]
68	0.72	−0.94	1.66	500(2.48)	310/370
69	0.71	−0.59	1.30	576(2.15)	280/570

[a] Measured by CV in acetonitrile *vs.* Ag/AgCl. [b] Measured in acetonitrile. [c] Static first order hyperpolarizability β_0 measured by HRS experiment (1300/800 nm lasers) in acetonitrile.

bands, highest calculated dipole moments and their changes upon excitation, as well as the largest NLO response. In this respect, the TCF acceptor imbues the π-conjugated backbone with the strongest electronic effects and, in combination with the proaromatic pyran-4-ylidene donor, significantly polarizes the whole molecule. This A/D combination yields the very efficient NLO phore **78** with a $\mu\beta_0$ value of 1520×10^{-48} esu.

The powerful accepting behavior of the TCF acceptor has further been investigated by Robinson *et al.*[92] They developed molecules **79** and **80** (Fig. 41), which have a ferrocene donor connected *via* a thienylenevinylene bridge to the TCF and CF_3-PhTCF acceptors. The electron withdrawing properties of the latter one were improved by attaching nonconjugated CF_3 and Ph groups. This relatively small but subtle structural change resulted in a significant red-shift of both high/low-energy (HE/LE) CT-bands and 1.2 times higher nonlinearity measured for **80**.

Acceptor variation as a powerful tool for tailoring the properties of simple thiophene-based chromophores **81–90** (Fig. 42), with prospective applications ranging from photorefractive (PR) materials to BHJ solar cells, has been shown by Würthner *et al.*[93,94]

Molecules **81–83**, **85–86** and **90** were applied as active materials in solution-processed BHJ solar cells, while the remaining ones were tested as PR materials (Table 26). In a series of indane-1,3-dione derived chromophores **81–83**, the electrochemical gap decreases steadily from 2.39 to 1.87 eV with increasing withdrawing ability of the acceptor moiety. This observation is also consistent with their CT-bands being red-shifted by 168 nm. Five- and six-membered heterocyclic moieties in **85–86** and **90** showed electrochemical gaps and positions of the longest-wavelength absorption maxima in a similar range as **82–83**. However, their ground-state dipoles are twice as large, whereas the change upon excitation is diminished. This implies

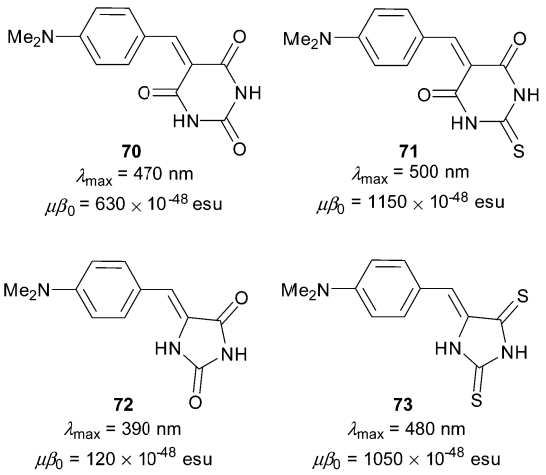

Fig. 39 Barbituric acid and related acceptors (all data were measured in DMSO (EFISH experiment at 1060 nm)).

that, in contrast to indane-1,3-dione acceptors in **81–83**, the structure of heterocyclic moieties in **85–86** and **90** (thiazole and tetrahydropyridine-2,6-dione derived) is shifted towards a zwitterionic character. OPVC devices based on these molecules and the $PC_{61}BM$ acceptor showed FF and power conversion efficiencies within the range 0.27–0.41 and 0.5–2.3%, respectively, with the highest performance measured for **82** bearing a 3-(dicyanomethylene)indan-1-one acceptor. Further optimization studies using this compound and different acceptors resulted in a device with power conversion efficiencies up to 4.5%.

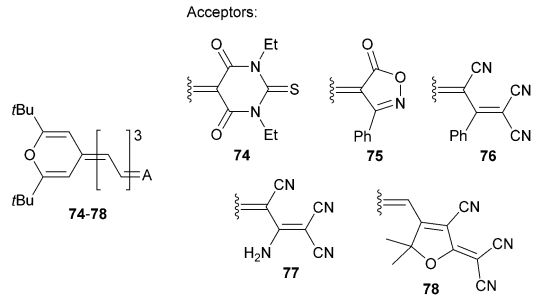

Fig. 40 Acceptor variation in push–pull molecules **74–78** bearing the proaromatic pyran-4-ylidene donor.

Table 25 Push–pull molecules **74–78**

Comp.	$E_{ox,1}$[a] [V]	$E_{red,1}$[a] [V]	E_g [eV]	λ_{max}[b] [nm (eV)]	$\mu/\Delta\mu$[c] [D]	$\mu\beta_0$[d] [10^{-48} esu]
74	0.83	−0.94	1.77	628(1.97)	11.4/2.2	300
75	0.77	−1.04	1.81	623(1.99)	10.8/2.4	380
76	0.88	−0.76	1.64	678(1.83)	16.4/5.6	670
77	0.87	−1.04	1.91	625(1.98)	16.1/6.6	360
78	0.68	−0.77	1.45	740(1.68)	17.8/7.1	1520

[a] Measured by CV in dichloromethane *vs.* Ag/AgCl. [b] Measured in dichloromethane. [c] Ground-state dipole moment and its change upon excitation (DFT calculation at the B3P86/6-31 G* level). [d] Measured by EFISH experiment (1907 nm) in dichloromethane.

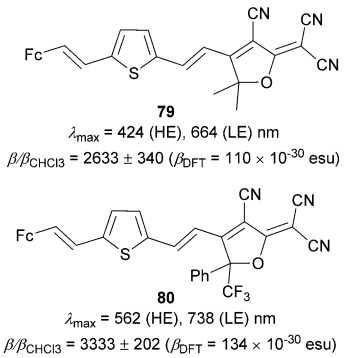

Fig. 41 Modification of TCF acceptor (all data were measured in chloroform (HRS experiment at 1000 nm).

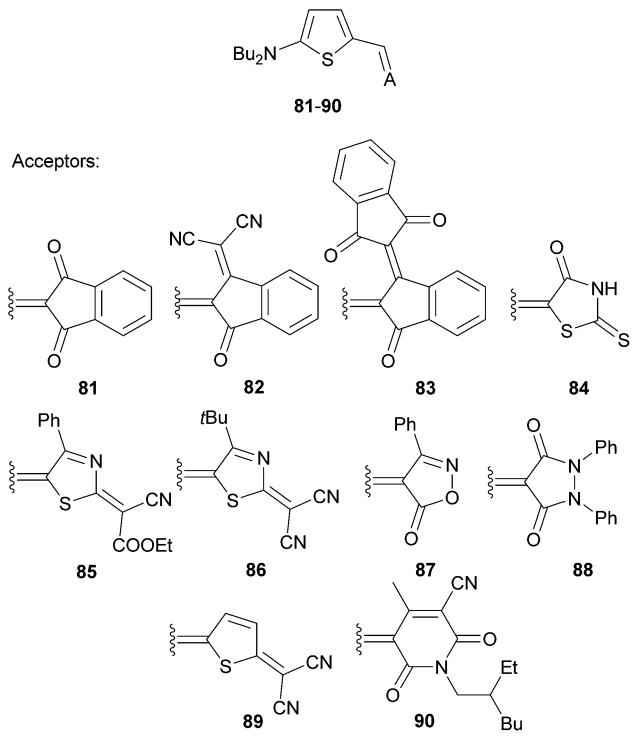

Fig. 42 Acceptor variation in push–pull molecules for PR materials and BHJ solar cells.

Chromophores **81**, **84** and **87–89** with indane-1,3-dione, thioxothiazolidinone, isoxazolone, pyrazolidinedione and thiophene derived acceptor units showed CT-bands around 500 nm (except for **89**) and generally lower ground-state dipole moments as compared to **85–86**. Whilst the photorefractive figures-of-merit F_0 of **81**, **84** and **87–88** are relatively low (~0.3), the thiophene based chromophore **89** showed a considerably higher dipole moment as well as $F_0 = 1.44$. Moreover, its narrow band absorption represents another significant advantage over the currently available PR chromophores and could lead to applications in optical laser devices.

7. Conclusions

In view of the current manifold applications of organic π-conjugated systems end-capped with electron donors and acceptors, understanding of their structure–property relationships seems to be crucial. Fundamental aspects of the property tuning in push–pull molecules summarized in this article are primarily aimed at the design of new D-π-A systems with improved/tailored properties such as FMO levels and electronic absorption/emission behaviour. The property tuning has been demonstrated by variations of particular D, π and A components of a push–pull molecule. The currently well-established and easily accessible electron donating groups involve aromatic amines (typically *N*,*N*-dimethylanilino (DMA), *N*,*N*-diphenylanilino (DPA), julolidine, carbazole), electron rich five-membered heterocycles such as thiophene or pyrrole (auxiliary donors), *N*,*N*-dialkylaminothiophene (typically piperidylthiophene (PIT)), tetrathiafulvalene (TTF) and metallocenes (typically ferrocene, dual donor). The main advantage of the amino-derived electron donors can be seen in their highly positive mesomeric effects (Table 1), synthetic availability and modularity and the possibility of a substitution with long alkyl chains, which supports good solubility of the chromophore (the eternal problem of push–pull molecules). Besides these "standard donors", proaromatic electron donors such as 4-pyran-4-ylidine, pyridine-4-ylidine and dithiafulvene were introduced in the early 90's. In a combination with strong acceptors, these

Table 26 PR and OPV properties of D–π–A systems **81–90**

Comp.	E_{HOMO}[a] [eV]	E_{LUMO}[a] [eV]	E_g [eV]	λ_{max} [nm (eV)]	$\mu/\Delta\mu$[b] [D]	F_0[c]	FF/η[d] [%]
81	−5.56	−3.17	2.39	532(2.33)[e]	5.7/4.2	0.24	0.27/0.5
82	−5.70	−3.56	2.14	595(2.08)[e]	8.6/4.1	—	0.41/2.3
83	−5.61	−3.74	1.87	700(1.77)[e]	6.1/4.6	—	0.36/1.0
84	—	—	—	513(2.42)[f]	6.7/7.2	0.32	—
85	−5.45	−3.55	1.90	689(1.80)[e]	12.1/2.3	—	0.27/0.5
86	−5.52	−3.62	1.90	682(1.82)[e]	13.1/2.5	—	0.35/1.1
87	—	—	—	500(2.48)[f]	7.9/2.4	0.35	—
88	—	—	—	489(2.54)[f]	7.0/2.1	0.26	—
89	—	—	—	647(1.92)[f]	11.2/7.8	1.44	—
90	−5.65	−3.36	2.29	556(2.23)[e]	12.6/1.7	—	0.32/0.9

[a] Measured by CV in dichloromethane *vs.* Fc/Fc^+. [b] Ground-state dipole moment and its change upon excitation (EOAM in dioxane). [c] PR figure-of-merit in 10^{-74} m^4 C^2 mol V^{-2} kg^{-1}. [d] Fill factor and power conversion efficiency. [e] Measured in thin film of the blend cast from chlorobenzene. [f] Measured in dichloromethane.

moieties impart very strong ICT into push–pull molecules. An overview of powerful electron donors is shown in Fig. 43.

Property tuning can also be achieved by varying the π-conjugated backbone connecting the D and A parts. The π-linker is most commonly constructed by a combination of multiple bonds and (hetero)aromatic units. Whereas the D–A interaction across a polyene is generally high, such D–π–A molecules often suffer from thermal/chemical instability and geometric isomerization. On the other hand, rod-like polyynes are more stable but "less transparent", due to the presence of more electronegative sp-hybridized carbons. A polarization of aromatic units (typically 1,4-phenylene unit) is accompanied by a loss of aromatic stabilization, which is directed against an efficient ICT. Hence, heteroaromatic/proaromatic units became more and more frequently employed as parts of the π-linker. In this respect, 2,5-thienylene and related spacers played very prominent role and became recognized as easily-accessible, polarizable and thus very popular π-conjugated bridges. In any case the overall performance of the given π-linker must be elucidated in terms of the D/A pair attached, its length, composition, planarity and degree of BLA.

As a matter of fact, electron withdrawing groups in push–pull molecules are more diverse than electron donors. Besides the common cyano and nitro groups, the modern push–pull molecules are equipped with more complex withdrawing moieties (Fig. 44). For instance, replacing the cyano by dicyanovinyl (DCV) acceptor groups may shift the longest-wavelength absorption maxima by more than 100 nm and narrowed the HOMO–LUMO gap by up to 1 eV. Malonic acid-derived acceptors such as DCV, cyanoacetic (cyanoacrylic) acid or (thio)barbituric acids (BA and TBA) proved to be a very powerful family of acceptors used in NLO or OPV devices. 1,3-Dicarbonyl compounds represent another more complex acceptor units. Indane-1,3-dione belongs to this type of acceptor, in which the withdrawing ability can further be tailored by appending one/two additional DCV units or a sulfoxide group. Moreover, both types of these acceptor units can be easily introduced *via* Knoevenagel condensation with donor-substituted carbonyl compounds.

In principle, almost all (hetero)aromatic scaffolds can be used as more or less efficient electron acceptors if properly substituted and arranged. The most widely employed are electron poor six-membered heterocycles such as (di)azines. Their electron accepting behaviour can be finely tuned by protonation, alkylation or (transition) metal coordination. Pyridinium and quaternized benzo[*d*]imidazole and benzo[*d*]thiazole derivatives are well known and easily available. However, the

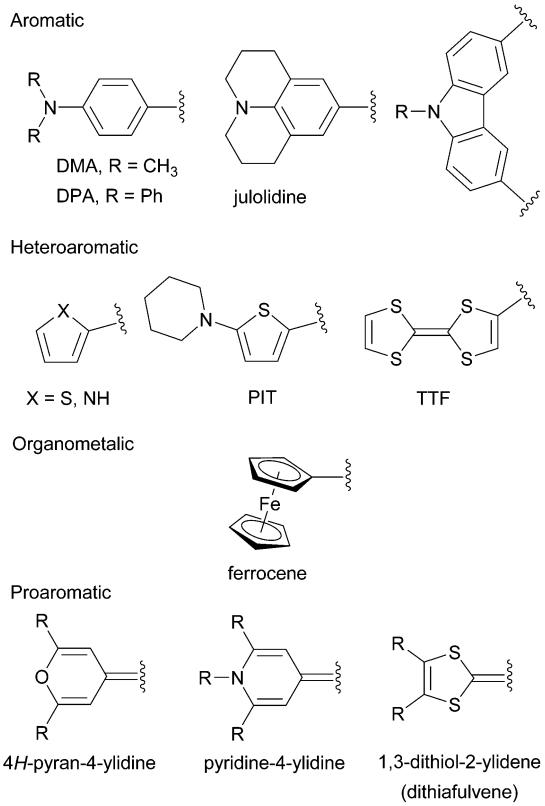

Fig. 43 Representative electron donors in push–pull molecules.

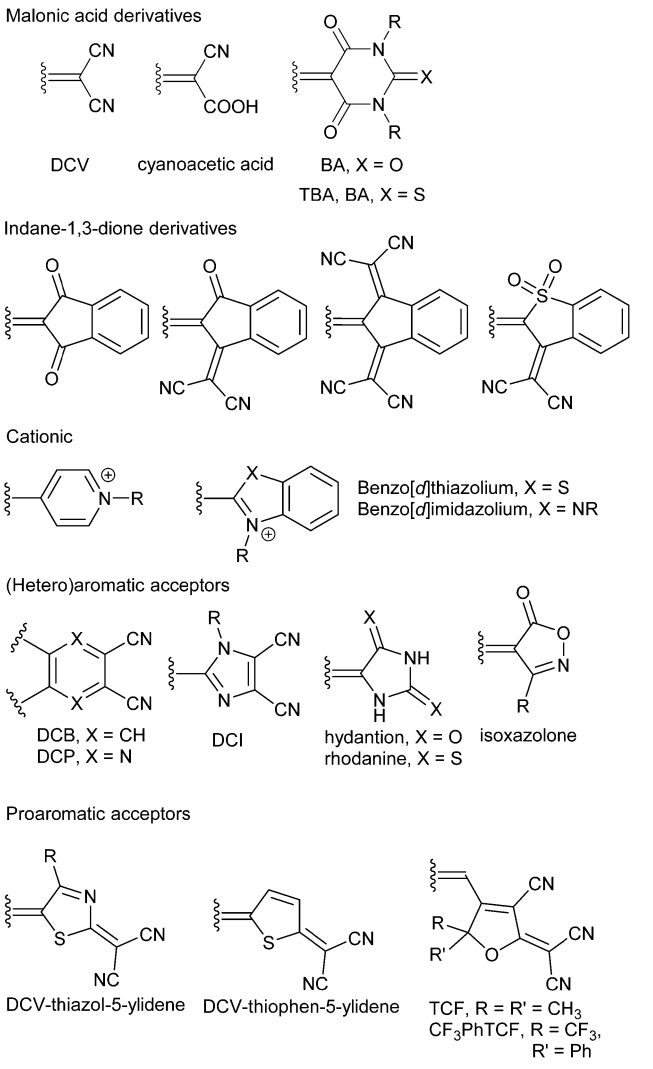

Fig. 44 Electron withdrawing moieties applied as acceptors in push–pull molecules.

ionic chromophore, with its solubility limited to only polar solvents, may represent an obstacle to its further (opto)electronic applications. We have recently introduced pyrazine/benzene-derived DCP/DCB electron acceptors on which X-shaped push–pull chromophores can be built. Dicyanoimidazole (DCI) can also be used in Y-shaped push–pull molecules, where it is considered as an acceptor with moderate withdrawing character. Five-membered heterocycles such as hydantoin and rhodanine are much powerful electron acceptors than imidazole. The chalcogen effect (O → S replacement) in these units is even more pronounced than in BA → TBA derivatives. The isoxazolone unit also showed a noticeable electron withdrawing ability. The DCV unit connected to a quinoid scaffold (typically benzoquionone) has been demonstrated as a powerful electron acceptor moiety a long time ago. However, appending the DCV unit to a heteroaromatic ring such as thiazol, thiophene or furan afforded a new class of very powerful proaromatic acceptors. These units showed considerably enhanced electron withdrawing ability compared to all preceding acceptors. The fine property tuning of the tricyanofuran (TCF) unit by subtle structural changes further enhances its accepting behaviour as shown by CF_3PhTCF.

Acknowledgements

This work was supported by the Czech Science Foundation (13-01061S). This review is dedicated to Prof. François Diederich who has introduced me to the fantastic world of push–pull molecules.

Notes and references

1 (*a*) Special issue on "Organic electronics and optoelectronics", ed. S. R. Forrest and M. E. Thompson, *Chem. Rev.*, 2007, **107**, 923; (*b*) Special issue on "Materials for electronics", ed. R. D. Miller and E. A. Chandross, *Chem. Rev.*, 2010, **110**, 1; (*c*) Special issue on "Molecular electronics – from a visionary concept towards reality", ed. M. Mayor, *Chimia*, 2010, **64**, 348.

2 Special issue on "Molecular conductors", ed. P. Batail, *Chem. Rev.*, 2004, **104**, 4887.

3 (*a*) Special issue on "Organic photovoltaics", ed. J. L. Bredas and J. R. Durrant, *Acc. Chem. Res.*, 2009, **42**, 1689; (*b*) Y. Lin, Y. Li and X. Zhan, *Chem. Soc. Rev.*, 2012, **41**, 4245.

4 Special issue on "Solar photon conversion", ed. A. J. Nozik and J. R. Miller, *Chem. Rev.*, 2010, **110**, 6443.

5 S. Allard, M. Forster, B. Souharce, H. Thiem and U. Scherf, *Angew. Chem., Int. Ed.*, 2008, **47**, 4070.

6 Y. Ohmori, *Laser Photonics Rev.*, 2009, **4**, 300.

7 A. W. Hains, Z. Liang, M. A. Woodhouse and B. A. Gregg, *Chem. Rev.*, 2010, **110**, 6689.

8 (*a*) Y. Wu and W. Zhu, *Chem. Soc. Rev.*, 2013, **42**, 2039; (*b*) J. N. Clifford, E. Martínez-Ferrero, A. Viterisi and E. Palomares, *Chem. Soc. Rev.*, 2011, **40**, 1635; (*c*) C. Duan, K. Zhang, C. Zhong, F. Huang and Y. Cao, *Chem. Soc. Rev.*, 2013, **42**, 9071; (*d*) M. Liang and J. Chen, *Chem. Soc. Rev.*, 2013, **42**, 3453.

9 C. Duan, F. Huang and Y. Cao, *J. Mater. Chem.*, 2012, **22**, 10416.

10 (*a*) M. Kivala and F. Diederich, *Acc. Chem. Res.*, 2009, **42**, 235; (*b*) S. Kato and F. Diederich, *Chem. Commun.*, 2010, **46**, 1994; (*c*) H. Meier, *Angew. Chem., Int. Ed.*, 2005, **44**, 2482; (*d*) M. Kivala and F. Diederich, *Pure Appl. Chem.*, 2008, **80**, 411.

11 *Handbook of thiophene-based materials, applications in organic electronics and photonics*, ed. I. F. Perepichka and D. F. Perepichka, Wiley, Chicester, 2009, vol. 1 and 2.

12 (*a*) R. Andreu, L. Carrasquer, S. Franco, J. Garín, J. Orduna, N. M. de Baroja, R. Alicante, B. Villacampa and M. Allain, *J. Org. Chem.*, 2009, **74**, 6647; (*b*) R. Andreu, E. Galán, J. Garín, V. Herrero, E. Lacarra, J. Orduna, R. Alicante and B. Villacampa, *J. Org. Chem.*, 2010, **75**, 1684; (*c*) N. Faux, B. Caro, F. Robin-Le Guen, P. Le Poul, K. Nakatani and E. Ishow, *J. Organomet. Chem.*, 2005, **690**, 4982; (*d*) S. Gauthier, N. Vologdin, S. Achelle, A. Barsella, B. Caro and F. Robin-Le Guen, *Tetrahedron*, 2013, **69**, 8392.

13 For reviews on metallocenes as donors see: (*a*) N. J. Long, *Angew. Chem., Int. Ed. Engl.*, 1995, **34**, 21; (*b*) H. S. Nalwa, *Appl. Organomet. Chem.*, 1991, **5**, 349.

14 (*a*) J. Kulhánek, F. Bureš, W. Kuznik, I. V. Kityk, T. Mikysek and A. Růžička, *Chem. - Asian J.*, 2013, **8**, 465; (*b*) S. Barlow, H. E. Bunting, C. Ringham, J. C. Green, G. U. Bublitz, S. G. Boxer, J. W. Perry and S. R. Marder, *J. Am. Chem. Soc.*, 1999, **121**, 3715; (*c*) S. Salman, J.-L. Brédas, S. R. Marder, V. Coropceanu and S. Barlow, *Organometallics*, 2013, **32**, 6061; (*d*) T. L. Kinnibrugh, S. Salman, Y. A. Getmanenko, V. Coropceanu, W. W. Porter III, T. V. Timofeeva, A. J. Matzger, J.-L. Brédas, S. R. Marder and S. Barlow, *Organometallics*, 2009, **28**, 1350.

15 (*a*) S. Achelle, C. Baudequin and N. Plé, *Dyes Pigm.*, 2013, **98**, 575; (*b*) S. Achelle, N. Plé and A. Turck, *RSC Adv.*, 2011, **1**, 364; (*c*) S. Achelle and N. Plé, *Curr. Org. Synth.*, 2012, **9**, 163.

16 (*a*) P. Hrobárik, V. Hrobáriková, I. Sigmundová, P. Zahradník, M. Fakis, I. Polyzos and P. Persephonis, *J. Org. Chem.*, 2011, **76**, 8726; (*b*) V. Hrobáriková, P. Hrobárik, P. Gajdoš, I. Fitilis, M. Fakis, P. Persephonis and P. Zahradník, *J. Org. Chem.*, 2010, **75**, 3053.

17 J. Kulhánek and F. Bureš, *Beilstein J. Org. Chem.*, 2012, **8**, 25.

18 (*a*) C. Hansch, A. Leo and R. W. Taft, *Chem. Rev.*, 1991, **91**, 165; (*b*) O. Pytela, *Collect. Czech. Chem. Commun.*, 1996, **61**, 704.

19 (*a*) M. A. Ramírez, A. M. Cuadro, J. Alvarez-Builla, O. Castaño, J. L. Andrés, F. Mendicuti, K. Clays, I. Asselberghs and J. J. Vaquero, *Org. Biomol. Chem.*, 2012, **10**, 1659; (*b*) M. A. Ramirez, T. Cañeque, A. M. Cuadro, F. Mendicuti, K. Clays, I. Asselbergh and J. J. Vaquero, *ARKIVOC*, 2011, **iii**, 140.

20 (*a*) W. Wu, C. Wang, C. Zhong, C. Ye, G. Qui, J. Qin and Z. Li, *Polym. Chem.*, 2013, **4**, 378; (*b*) J. Zhu, C. Lu, Y. Cui, C. Zhang and G. Lu, *J. Chem. Phys.*, 2010, **133**, 244503.

21 Benzene-derived X-shaped chromophores: (*a*) J. A. Marsden, J. J. Miller, L. D. Shirtcliff and M. M. Haley, *J. Am. Chem. Soc.*, 2005, **127**, 2464; (*b*) E. L. Spitler, L. D. Shirtcliff and M. M. Haley, *J. Org. Chem.*, 2007, **72**, 86; (*c*) D. T. Chase, B. S. Young and M. M. Haley, *J. Org. Chem.*, 2011, **76**, 4043;

(*d*) H. Kang, G. Evmenenko, P. Dutta, K. Clays, K. Song and T. J. Marks, *J. Am. Chem. Soc.*, 2006, **128**, 6194.

22 Ethene-derived X-shaped chromophores: (*a*) N. K. Pahadi, D. H. Camacho, I. Nakamura and Y. Yamamoto, *J. Org. Chem.*, 2006, **71**, 1152; (*b*) N. N. P. Moonen, C. Boudon, J.-P. Gisselbrecht, P. Seiler, M. Gross and F. Diederich, *Angew. Chem., Int. Ed.*, 2002, **41**, 3044; (*c*) N. N. P. Moonen, W. C. Pomerantz, R. Gist, C. Boudon, J.-P. Gisselbrecht, T. Kawai, A. Kishioka, M. Gross, M. Irie and F. Diederich, *Chem. - Eur. J.*, 2005, **11**, 3325; (*d*) F. Bureš, W. B. Schweizer, J. C. May, C. Boudon, J.-P. Gisselbrecht, M. Gross, I. Biaggio and F. Diederich, *Chem. - Eur. J.*, 2007, **13**, 5378.

23 Heteroaromate-derived X-shaped chromophores: (*a*) F. Bureš, H. Čermáková, J. Kulhánek, M. Ludwig, W. Kuznik, I. V. Kityk, T. Mikysek and A. Růžička, *Eur. J. Org. Chem.*, 2012, 529; (*b*) Y. Zhao, C. Zhang, K. F. Chin, O. Pytela, G. Wei, H. Liu, F. Bureš and Z. Jiang, *RSC Adv.*, 2014, **4**, 30062.

24 (*a*) Special issue on "Optical nonlinearities in chemistry", ed. D. Burland, *Chem. Rev.*, 1994, **94**, 1; (*b*) G. S. He, L.-S. Tan, Q. Zheng and P. N. Prasad, *Chem. Rev.*, 2008, **108**, 1245; (*c*) Y. Kawabe, H. Ikeda, T. Sakai and K. Kawasaki, *J. Mater. Chem.*, 1992, **2**, 1025; (*d*) S. R. Marder and J. W. Perry, *Adv. Mater.*, 1993, **5**, 804.

25 (*a*) P. A. Sullivan and L. R. Dalton, *Acc. Chem. Res.*, 2010, **43**, 10; (*b*) M. Stähelin, B. Zysset, M. Ahlheim, S. R. Marder, P. V. Bedworth, C. Runser, M. Barzoukas and A. Fort, *J. Opt. Soc. Am. B*, 1996, **13**, 2401.

26 F. Chen, J. Zhang and X. Wan, *Chem. - Eur. J.*, 2012, **18**, 4558.

27 (*a*) B. J. Coe, *Chem. - Eur. J.*, 1999, **5**, 2464; (*b*) I. Asselberghs, K. Clays, A. Persoons, M. D. Ward and J. McCleverty, *J. Mater. Chem.*, 2004, **14**, 2831.

28 F. M. Raymo and M. Tomasulo, *Chem. - Eur. J.*, 2006, **12**, 3186.

29 (*a*) C. Reichardt, *Solvents and solvent effects in organic chemistry*, Wiley-VCH, Weinheim, 2004; (*b*) F. Bureš, O. Pytela, M. Kivala and F. Diederich, *J. Phys. Org. Chem.*, 2011, **24**, 274; (*c*) F. Bureš, O. Pytela and F. Diederich, *J. Phys. Org. Chem.*, 2009, **22**, 155.

30 (*a*) M. G. Kuzyk, *J. Mater. Chem.*, 2009, **19**, 7444; (*b*) Y. Sheng, Y. Jiang and X.-C. Wang, *J. Chem. Soc., Faraday Trans.*, 1998, **94**, 47; (*c*) J. Y. Lee, K. S. Kim and B. J. Mhin, *J. Chem. Phys.*, 2001, **115**, 9484; (*d*) T. Le Bahers, C. Adamo and I. Ciofini, *J. Chem. Theory Comput.*, 2011, **7**, 2498; (*e*) A. Datta and S. Pal, *THEOCHEM*, 2005, **715**, 59; (*f*) F. Bureš, *Chem. Listy*, 2013, **107**, 834.

31 (*a*) J. Roncali, *Macromol. Rapid Commun.*, 2007, **28**, 1761; (*b*) J. Roncali, *Chem. Rev.*, 1997, **97**, 173; (*c*) H. A. M. van Mullekom, J. A. J. M. Vekemans, E. E. Havinga and E. W. Meijer, *Mater. Sci. Eng., R*, 2001, **32**, 1; (*d*) D. F. Perepichka and M. R. Bryce, *Angew. Chem., Int. Ed.*, 2005, **44**, 5370.

32 J. Kulhánek, F. Bureš, O. Pytela, T. Mikysek, J. Ludvík and A. Růžička, *Dyes Pigm.*, 2010, **85**, 57.

33 J. Kulhánek, F. Bureš and M. Ludwig, *Beilstein J. Org. Chem.*, 2009, **5**, 11.

34 A. A. Isse and A. Gennaro, *J. Phys. Chem. B*, 2010, **114**, 7894.

35 J. Kulhánek, F. Bureš, A. Wojciechowski, M. Makowska-Janusik, E. Gondek and I. V. Kityk, *J. Phys. Chem. A*, 2010, **114**, 9440.

36 F. Würthner, F. Effenberger, R. Wortmann and P. Krämer, *Chem. Phys.*, 1993, **173**, 305.

37 (*a*) A. E. Stiegman, E. Graham, K. J. Perry, L. R. Khundkar, L.-T. Cheng and J. W. Perry, *J. Am. Chem. Soc.*, 1991, **113**, 7658; (*b*) C. Dehu, F. Meyers and J. L. Brédas, *J. Am. Chem. Soc.*, 1993, **115**, 6198.

38 S. R. Marder, L.-T. Cheng and B. G. Tiemann, *J. Chem. Soc., Chem. Commun.*, 1992, 672.

39 (*a*) L.-T. Cheng, W. Tam, S. H. Stevenson, G. R. Meredith, G. Rikken and S. R. Marder, *J. Phys. Chem.*, 1991, **95**, 10631; (*b*) L.-T. Cheng, W. Tam, S. R. Marder, A. E. Stiegman, G. Rikken and C. W. Spangler, *J. Phys. Chem.*, 1991, **95**, 10643; (*c*) S. R. Marder, C. B. Gorman, B. G. Tiemann and L.-T. Cheng, *J. Am. Chem. Soc.*, 1993, **115**, 3006; (*d*) G. Bourhill, J.-L. Brédas, L.-T. Cheng, S. R. Marder, F. Meyers, J. W. Perry and B. G. Tiemann, *J. Am. Chem. Soc.*, 1994, **116**, 2619.

40 (*a*) M. Blanchard-Desce, V. Alain, P. V. Bedworth, S. R. Marder, A. Fort, C. Runser, M. Barzoukas, S. Lebus and R. Wortmann, *Chem. - Eur. J.*, 1997, **3**, 1091; (*b*) E. Genin, V. Hugues, G. Clermont, C. Herbivo, M. C. R. Castro, A. Comel, M. M. M. Raposo and M. Blanchard-Desce, *Photochem. Photobiol. Sci.*, 2012, **11**, 1756.

41 A. Abbotto, L. Beverina, R. Bozio, S. Bradamante, C. Ferrante, G. A. Pagani and R. Signorini, *Adv. Mater.*, 2000, **12**, 1963.

42 J. Zhang, L. Yang, M. Zhang and P. Wang, *RSC Adv.*, 2013, **3**, 6030.

43 R. Tarsang, V. Promarak, T. Sudyoadsuk, S. Namuangruk and S. Jungsuttiwong, *J. Photochem. Photobiol., A*, 2014, **273**, 8.

44 M.-B. S. Kirketerp, M. Å. Petersen, M. Wanko, H. Zettergren, A. Rubio, M. B. Nielsen and S. B. Nielsen, *ChemPhysChem*, 2010, **11**, 2495.

45 (*a*) M. Makowska-Janusik, I. V. Kityk, J. Kulhánek and F. Bureš, *J. Phys. Chem. A*, 2011, **115**, 12251; (*b*) A. Plaquet, B. Champagne, J. Kulhánek, F. Bureš, E. Bogdan, F. Castet, L. Ducasse and V. Rodriguez, *ChemPhysChem*, 2011, **12**, 3245; (*c*) N. Almonasy, F. Bureš, J. Kulhánek and O. Machalický, *J. Mater. Sci. Eng. A*, 2011, **1**, 146; (*d*) M. Nepraš, N. Almonasy, F. Bureš, J. Kulhánek, M. Dvořák and M. Michl, *Dyes Pigm.*, 2011, **91**, 466; (*e*) M. Danko, P. Hrdlovič, J. Kulhánek and F. Bureš, *J. Fluoresc.*, 2011, **21**, 1779; (*f*) F. Bureš, J. Kulhánek, T. Mikysek, J. Ludvík and J. Lokaj, *Tetrahedron Lett.*, 2010, **51**, 2055.

46 (*a*) S. Yang and M. Kertesz, *J. Phys. Chem. A*, 2006, **110**, 9771; (*b*) D. Jacquemin and C. Adamo, *J. Chem. Theory Comput.*, 2011, **7**, 369; (*c*) M. Medveď and D. Jacquenim, *Chem. Phys.*, 2013, **415**, 196; (*d*) C. Maertens, C. Detrembleur, P. Dubois, R. Jérôme, C. Boutton, A. Persoons, T. Kogej and J. L. Brédas, *Chem. - Eur. J.*, 1999, **5**, 369.

47 A. M. Moran, M. Blanchard-Desce and A. M. Kelly, *Chem. Phys. Lett.*, 2002, **358**, 320.

48 J. Garín, J. Orduna, J. I. Rupérez, R. Alcalá, B. Villacampa, C. Sánchez, N. Martín, J. L. Segura and M. Gonzáles, *Tetrahedron Lett.*, 1998, **39**, 3577.
49 C. R. Moylan, R. J. Twieg, V. Y. Lee, S. A. Swanson, K. M. Betterton and R. D. Miller, *J. Am. Chem. Soc.*, 1993, **115**, 12599.
50 C. Coluccini, A. K. Sharma, M. Caricato, A. Sironi, E. Cariati, S. Righetto, E. Tordin, C. Botta, A. Forni and D. Pasini, *Phys. Chem. Chem. Phys.*, 2013, **15**, 1666.
51 J. C. May, I. Baggio, F. Bureš and F. Diederich, *Appl. Phys. Lett.*, 2007, **90**, 251106.
52 E. Zojer, D. Beljonne, P. Pacher and J.-L. Brédas, *Chem. - Eur. J.*, 2004, **10**, 2668.
53 (*a*) I. D. L. Albert, T. J. Marks and M. A. Ratner, *J. Am. Chem. Soc.*, 1997, **119**, 6575; (*b*) S. Bradamante, A. Facchetti and G. A. Pagani, *J. Phys. Org. Chem.*, 1997, **10**, 514; (*c*) J. L. Brédas, *J. Chem. Phys.*, 1985, **82**, 3808.
54 J. Kulhánek, F. Bureš, J. Opršal, W. Kuznik, T. Mikysek and A. Růžička, *Asian J. Org. Chem.*, 2013, **2**, 422.
55 (*a*) A. K.-Y. Jen, V. P. Rao, K. Y. Wong and K. J. Drost, *J. Chem. Soc., Chem. Commun.*, 1993, 90; (*b*) V. P. Rao, Y. M. Cai and A. K.-Y. Jen, *J. Chem. Soc., Chem. Commun.*, 1994, 1689.
56 K. Y. Wong, A. K.-Y. Jen, V. P. Rao and K. J. Drost, *J. Chem. Phys.*, 1994, **100**, 6818.
57 C. R. Moylan, B. J. McNelis, L. C. Nathan, M. A. Marques, E. L. Hermstadt and B. A. Brichler, *J. Org. Chem.*, 2004, **69**, 8239.
58 (*a*) M. M. Oliva, J. Casado, M. M. M. Raposo, A. M. C. Fonseca, H. Hartmann, V. Hernández and J. T. L. Navarrete, *J. Org. Chem.*, 2006, **71**, 7509; (*b*) M. M. M. Raposo and G. Kirsch, *Tetrahedron*, 2003, **59**, 4891; (*c*) M. M. M. Raposo, A. M. C. Fonseca and G. Kirsch, *Tetrahedron*, 2004, **60**, 4071; (*d*) A. Wojciechowski, M. M. M. Raposo, M. C. R. Castro, W. Kuznik, I. Fuks-Janczarek, M. Pokladko-Kowar and F. Bureš, *J. Mater. Sci.: Mater. Electron.*, 2014, **25**, 1745.
59 P. V. Bedworth, Y. Cai, A. Jen and S. R. Marder, *J. Org. Chem.*, 1996, **61**, 2242.
60 I. D. L. Albert, T. J. Marsk and M. A. Ratner, *J. Am. Chem. Soc.*, 1997, **119**, 6575.
61 P. R. Varanasi, A. K.-Y. Jen, J. Chandrasekhar, I. N. N. Namboothiri and A. Rathna, *J. Am. Chem. Soc.*, 1996, **118**, 12443.
62 B. O'Regan and M. Grätzel, *Nature*, 1991, **353**, 737.
63 D. Casanova, *ChemPhysChem*, 2011, **12**, 2979.
64 D. P. Hagberg, T. Marinado, K. M. Karlsson, K. Nonomura, P. Qin, G. Boschloo, T. Brinck, A. Hagfeldt and L. Sun, *J. Org. Chem.*, 2007, **72**, 9550.
65 (*a*) S. H. Kim, H. W. Kim, C. Sakong, J. Namgoong, S. W. Park, M. J. Ko, C. H. Lee, W. I. Lee and J. P. Kim, *Org. Lett.*, 2011, **13**, 5784; (*b*) H. Tian, X. Yang, R. Chen, Y. Pan, L. Li, A. Hagfeldt and L. Sun, *Chem. Commun.*, 2007, 3741.
66 R. Li, X. Lv, D. Shi, D. Zhou, Y. Cheng, G. Zhang and P. Wang, *J. Phys. Chem. C*, 2009, **113**, 7469.
67 S. R. Marder, D. N. Beratan and L.-T. Cheng, *Science*, 1991, **252**, 103.
68 *Characterization techniques and tabulations for organic nonlinear optical materials*, ed. M. G. Kuzyk and C. W. Dirk, Marcel Dekker, New York, 1998.
69 (*a*) Y.-L. Wu, F. Bureš, P. D. Jarowski, W. B. Schweizer, C. Boudon, J.-P. Gisselbrecht and F. Diederich, *Chem. - Eur. J.*, 2010, **16**, 9592; (*b*) F. Bureš, W. B. Schweizer, C. Boudon, J.-P. Gisselbrecht, M. Gross and F. Diederich, *Eur. J. Org. Chem.*, 2008, 994.
70 T. Kawase, M. Wakabayashi, C. Takahashi and M. Oda, *Chem. Lett.*, 1997, 1055.
71 A. J. Kay, A. D. Woolhouse, Y. Zhao and K. Clays, *J. Mater. Chem.*, 2004, **14**, 1321.
72 A. Abbotto, L. Beverina, S. Bradamante, A. Fachetti, C. Klein, G. A. Pagani, M. Redi-Abshiro and R. Wortmann, *Chem. - Eur. J.*, 2003, **9**, 1991.
73 S. Alías, R. Andreu, M. J. Blesa, S. Franco, J. Garín, A. Gragera, J. Orduna, P. Romero, B. Villacampa and M. Allain, *J. Org. Chem.*, 2007, **72**, 6440.
74 R. Andreu, M. A. Cerdán, S. Franco, J. Garín, A. B. Marco, J. Orduna, D. Palomas, B. Villacampa, R. Alicante and M. Allain, *Org. Lett.*, 2008, **10**, 4963.
75 R. Andreu, E. Galán, J. Orduna, B. Villacampa, R. Alicante, J. T. L. Navarrete, J. Casado and J. Garín, *Chem. - Eur. J.*, 2011, **17**, 826.
76 (*a*) R. Gompper, E. Kutter and H.-U. Wagner, *Angew. Chem., Int. Ed. Engl.*, 1966, **5**, 517; (*b*) R. Gompper, H.-U. Wagner and E. Kutter, *Chem. Ber.*, 1968, **101**, 4123.
77 S. Inoue, Y. Aso and T. Otsubo, *Chem. Commun.*, 1997, 1105.
78 S. Inoue, S. Mikami, Y. Aso, T. Otsubo, T. Wada and H. Sasabe, *Synth. Met.*, 1997, **84**, 395.
79 A. S. Batsanov, M. R. Bryce, M. A. Coffin, A. Green, R. E. Hester, J. A. K. Howard, I. K. Lednev, N. Martín, A. J. Moore, J. N. Moore, E. Ortí, L. Sánchez, M. Savirón, P. M. Viruela, R. Viruela and T.-Q. Ye, *Chem. - Eur. J.*, 1998, **4**, 2580.
80 R. Andreu, J. Garín, J. Orduna, R. Alcalá and B. Villacampa, *Org. Lett.*, 2003, **5**, 3143.
81 S. Alías, R. Andreu, M. J. Blesa, M. A. Cerdán, S. Franco, J. Garín, C. López, J. Orduna, J. Sanz, R. Alicante, B. Villacampa and M. Allain, *J. Org. Chem.*, 2008, **73**, 5890.
82 R. Andreu, M. J. Blesa, L. Carrasquer, J. Garín, J. Orduna, B. Villacampa, R. Alcalá, J. Casado, M. C. R. Delgado, J. T. L. Navarrete and M. Allain, *J. Am. Chem. Soc.*, 2005, **127**, 8835.
83 M. G. Vivas, D. L. Silva, J. Malinge, M. Boujtita, R. Zaleśny, W. Bartkowiak, H. Ågren, S. Canuto, L. De Boni, E. Ishow and C. R. Mendonca, *Sci. Rep.*, 2014, **4**, 4447.
84 C. Herbivo, A. Comel, G. Kirsch, A. M. C. Fonseca, M. Belsley and M. M. M. Raposo, *Dyes Pigm.*, 2010, **86**, 217.
85 J.-M. Raimundo, P. Blanchard, I. Ledoux-Rak, R. Hierle, L. Michaux and J. Roncali, *Chem. Commun.*, 2000, 1597.
86 L. Dokládalová, F. Bureš, W. Kuznik, I. V. Kityk, A. Wojciechowski, T. Mikysek, N. Almonasy, M. Ramaiyan, Z. Padělková, J. Kulhánek and M. Ludwig, *Org. Biomol. Chem.*, 2014, **12**, 5517.

87 M. Klikar, F. Bureš, O. Pytela, T. Mikysek, Z. Padělková, A. Barsella, K. Dorkenoo and S. Achelle, *New J. Chem.*, 2013, **37**, 4230.
88 S. Achelle, S. Kahlal, A. Barsella, J.-Y. Saillard, X. Che, J. Vallet, F. Bureš, B. Caro and F. Robin-le Guen, *Dyes Pigm.*, 2015, **113**, 562.
89 B. J. Coe, J. A. Harris, J. J. Hall, B. S. Brunschwig, S.-T. Hung, W. Libaers, K. Clays, S. J. Coles, P. N. Horton, M. E. Light, M. B. Hursthouse, J. Garín and J. Orduna, *Chem. Mater.*, 2006, **18**, 5907.
90 F. Quist, C. M. L. Vande Velde, D. Didier, A. Teshome, I. Asselberghs, K. Clays and S. Sergeyev, *Dyes Pigm.*, 2009, **81**, 203.
91 H. Ikeda, Y. Kawabe, T. Sakai and K. Kawasaki, *Chem. Lett.*, 1989, 1803.
92 Y. Liao, B. E. Eichinger, K. A. Firestone, M. Haller, J. Luo, W. Kaminsky, J. B. Benedict, P. J. Reid, A. K.-Y. Jen, L. R. Dalton and B. H. Robinson, *J. Am. Chem. Soc.*, 2005, **127**, 2758.
93 F. Würthner, C. Thalacker, R. Matschiner, K. Lukaszuk and R. Wortmann, *Chem. Commun.*, 1998, 1739.
94 H. Bürckstümmer, E. V. Tulyakova, M. Deppisch, M. R. Lenze, N. M. Kronenberg, M. Gsänger, M. Stolte, K. Meerholz and F. Würthner, *Angew. Chem., Int. Ed.*, 2011, **50**, 11628.